Journal Pre-proofs

Mechanistic investigations in ultrasound–assisted biodegradation of phenanthrene

Niharika Kashyap, Kuldeep Roy, Vijayanand S. Moholkar

PII: S1350-4177(19)31572-X
DOI: https://doi.org/10.1016/j.ultsonch.2019.104890
Reference: ULTSON 104890

To appear in: *Ultrasonics Sonochemistry*

Received Date: 7 October 2019
Revised Date: 18 November 2019
Accepted Date: 19 November 2019

Please cite this article as: N. Kashyap, K. Roy, V.S. Moholkar, Mechanistic investigations in ultrasound–assisted biodegradation of phenanthrene, *Ultrasonics Sonochemistry* (2019), doi: https://doi.org/10.1016/j.ultsonch.2019.104890

Mechanistic investigations in ultrasound–assisted biodegradation of phenanthrene

Niharika Kashyap[1], Kuldeep Roy[2], and Vijayanand S. Moholkar[1,2,*]

[1] Centre for the Environment, [2] Department of Chemical Engineering

Indian Institute of Technology Guwahati

Guwahati – 781 039, Assam, India

* Author for correspondence. E–mail: vmoholkar@iitg.ac.in, Fax: +91 361 258 2291

Abstract

This study has addressed the biodegradation of polycyclic aromatic hydrocarbon, phenanthrene using *Candida tropicalis*. Optimization using central composite statistical design yielded optimum experimental parameters as: pH = 6.2, temperature = 33.4°C, mechanical shaking = 190 rpm and % inoculum = 9.26% v/v. Sonication of biodegradation mixture at 33 kHz and 10% duty cycle in log phase (12 h per day for 4 days) resulted in a 25% enhancement in phenanthrene removal. Profiles of specific growth rate (μ) and specific degradation rate (q) versus initial substrate concentration were fitted to Haldane substrate inhibition model. Both μ and q showed maxima for initial concentration of 100 mg L^{-1}. Kinetic analysis of degradation profiles showed higher biomass yield coefficient and smaller decay coefficient in presence of sonication. Expression of total intracellular proteins in control and test experiments were analyzed using SDS–PAGE. This analysis revealed overexpression of enzyme catechol 2,3–dioxygenase (in *meta* route metabolism) during sonication which is involved in ring cleavage of phenanthrene. Evaluation of cell viability after sonication by flow cytometry analysis revealed >80% live cells. These effects are attributed to enhanced cellular transport induced by intense microturbulence generated by sonication.

Keywords: Polycyclic aromatic hydrocarbons; *Candida tropicalis*; Phenanthrene; Biodegradation; Haldane kinetic model; Ultrasound

1. Introduction

Polycyclic aromatic hydrocarbons (PAHs) appearing in discharges from chemical and process industries, have gained noteworthy attention for decades due their extraordinary stability in terrestrial/aquatic environments, resistance to degradation through conventional advanced oxidation processes (AOPs) and harmful effects on ecosystem [1], [2]. Bioremediation of PAHs has emerged as a potential alternative to conventional oxidative processes. Several ligninolytic or non–ligninolytic fungi have been employed for bioremediation [3], [4], [5], [6]. However, for bioremediation of wastewater, non–ligninolytic fungi are more suitable, since the ligninolytic fungi have habitat limitation of growth [7]. The most commonly used non–ligninolytic fungi for bioremediation of PAH belong to genera *Candida*, *Fusarium*, *Aspergillus*, *Penicillium,* and *Pichia* [8], [9], [10]. Microbial degradation route of PAHs by non–ligninolytic fungi normally comprises of three phases, viz. (a) activation of aromatic ring, (b) dearomatization, (c) transformation of ring fission products into tricarboxylic acid (TCA) cycle metabolites. A normal pathway of metabolic cleavage of PAH comprises of dihydroxylation of benzene ring into catechol derivative and then ring fission via *ortho* (intradiol) or *meta* (extradiol) oxidation route. Catechol undergoes oxidation either by cleavage enzyme catechol 1,2– dioxygenase (C1,2–D) to form *cis, cis*–muconic acid through *ortho*– route. Aletrantively, catechol may also be oxidised by cleavage enzyme catechol 2,3–dioxygenase (C2,3–D) through *meta*– route resulting in formation of 2–hydroxymuconic semialdehyde (HMSA) [11]. A brief review of representative literature on degradation of different PAHs is provided in Table 1. It could be inferred that the degradation kinetics of PAHs by different microbial strains is quite slow. Moreover, many yeasts need to be supplemented with additional carbon source, surfactants and other additives such as yeast extract.

The degrading capability of microorganisms also depends on physical parameters like pH, carbon sources, temperature, and nutrients [12]. Biodegradation of PAHs can be enhanced by proper optimization of the physical process parameters [13], [14]. Bioremediation can also be coupled with other techniques of process intensification. One of the contemporary techniques, for enhancing

kinetics/yields of biochemical processes is ultrasound irradiation or sonication [15]. Previous authors have coupled sonication with inorganic catalysts for boosting the kinetics of degradation of organic pollutants [16], [17]. Sonication of moderate intensity is known to augment the kinetics of the bioprocesses. Physical and chemical effects of sonication are responsible for intensification of the process. The phenomenon of cavitation (growth, nucleation, and the transient collapse of bubble) is responsible for the physical/chemical effects of sonication. The major physical effect produced by sonication is intense microturbulence in the system, and the chemical effect is formation of highly reactive radicals through thermal dissociation of gas and vapor molecules in the cavitation bubble.

In this study, we have attempted to investigate ultrasound–assisted biodegradation of PAHs from a mechanistic viewpoint. The model system of present study comprises of phenanthrene and *Candida tropicalis* MTCC 184. The present study begins with statistical optimization of degradation parameters followed by experiments on ultrasound–assisted degradation at optimum conditions. The experimental profiles of biomass and substrate during bioremediation have been analysed using kinetic models that account for substrate inhibition. The predominant metabolic pathway of phenanthrene degradation has been identified in mechanical shaking (control) and with sonication (test). Moreover, over–expression of cellular proteins during sonication were also assessed using SDS–PAGE analysis. Concurrent analysis of these studies has revealed interesting mechanistic aspects of ultrasound–induced enhancement of phenanthrene biodegradation by *C. tropicalis* cells. Finally, the effect of sonication on cell viability and morphology has been assessed.

2. Materials and methods

2.1. Microbial growth and maintenance

Yeast strain, *C. tropicalis* MTCC 184, was acquired from the Institute of Microbial Technology (IMTECH), Chandigarh, India. The yeast strain was conserved by sub–culturing on yeast extract peptone dextrose (YEPD) agar plates and storage at 4°C. Sub–culture was done every

month and preserved at –80°C in glycerol (20% v/v). The culture was grown at 30°C, 150 rpm agitation, and pH 7. For PAH biodegradation, the yeast was grown in Bushnell–Hass (BH) minimal salt medium (MSM) with a composition of (g L^{-1}): K_2HPO_4 (1.0); KH_2PO_4 (1.0); NH_4NO_3 (1.0); $FeCl_3$ (0.05); $MgSO_4 \cdot 7H_2O$ (0.2) and $CaCl_2 \cdot 2H_2O$ (0.02). The biodegradation experiments were performed in BH medium with phenanthrene (PAH) as sole carbon source.

2.2. Chemicals, medium, and reagents

Phenanthrene (sublimed grade, ≥ 99.5%) was procured from Sigma–Aldrich (India). Bushnell Haas medium (BHM) was procured from Himedia (Mumbai, India). HPLC grade acetonitrile, acetone, and n–hexane were purchased from Merck, India. The rest of the chemicals (analytical grade) used for analysis were acquired from Himedia (Mumbai, India).

2.3. Biodegradation experiments

In a typical experiment, the yeast culture was initially grown in YEPD medium at 30°C, 150 rpm agitation and pH 7. The pre–culture was incubated until it attained an optical density of 0.5 – 0.6 at 600 nm (OD600 nm). Successively, yeast biomass was separated through centrifugation, washed, and the pellets were suspended in BH medium. Next, the pre–culture was inoculated in the degradation medium with phenanthrene (PAH) as the sole carbon source. Prior to degradation, BH medium was sterilized (autoclaved at 121°C, 20 min) followed by inoculation of seed culture. Phenanthrene has negligible solubility in pure water. Hence, 10 mg phenanthrene was dissolved in minimum acetone (2 – 3 mL), and this mixture was added to working volume of 100 mL BHM. Thus, the phenanthrene concentration in resulting solution is ~ 100 mg L^{-1}. Un–inoculated controls flasks containing only BHM and phenanthrene were maintained to validate any abiotic loss. The experiments were carried out for 14 days and samples of the reaction mixture were collected at regular intervals to monitor cell biomass growth and residual phenanthrene.

After completion of 14-day experiment, samples were initially extracted using an equal volume of n–hexane. The mixtures were vortex agitated, followed by 10 min centrifugation (10,000 rpm) to transfer residual phenanthrene in the organic layer. The solution was allowed to settle, and the organic layer comprising n–hexane, and phenanthrene was procured in vials. Samples with three replicates were prepared and were analyzed using high performance liquid chromatography (HPLC, Agilent Technologies, 1220 Infinity LC) fitted with C18 reverse–phase column (3 mm ×150 mm and particle size of 3.5 μm). Mixture of acetonitrile: milli–Q water (volume ratio 70:30) was used as the mobile phase (or eluent). The sample injection volume was 20 μL and flow rate of mobile phase was 0.8 mL min^{-1} flow rate. Phenanthrene was identified with a UV detector (254 nm), and retention time was compared against standards of phenanthrene.

2.4. Statistical optimization of phenanthrene degradation

The physical parameters related to phenanthrene biodegradation were optimized by response surface methodology using the central composite design of experiments. Four experimental parameters, viz. medium pH, % inoculum, temperature, and mechanical shaking, were taken as the independent variables (or optimization parameters). Percentage degradation of phenanthrene was the response (or dependent) variable. The notations for optimization parameters (or factors) and their levels (with actual and coded values) are provided in Table 2. The complete design of 31 experiments (MINITAB, Trial version) was based on five coded levels ($-\alpha$, –1, 0, +1, $+\alpha$) of optimization parameters. This is provided in supplementary material. The results of statistical experimental design were analysed using response surface methodology.

The experimental data acquired from central composite design (provided in supplementary material) was fitted to the quadratic equation with individual and interactive coefficients corresponding to optimization parameters:

$$Y = \beta_0 + \sum_{i=1}^{k} \beta_i X_i + \sum_{i=1}^{k} \beta_{ii} X_i^2 + \sum \sum \beta_{ij} X_i X_j \quad (1)$$

Notation: Y − dependent variable (% PAH degraded), k − number of factors, $\beta_0, \beta_i, \beta_{ii}, \beta_{ij}$ − regression coefficient acquired for constant, linear, quadratic, and interaction, respectively. The coded values (X) of the optimization parameters are defined as: $X = (x_i - x_0)/\Delta x$, where i = 1, 2, 3…, x_i is a dimensionless value of the variables, x_0 is the value of x_i at center point, and Δx is the step change.

***Validation (or control) experiments*:** For validation of statistical optimization, phenanthrene biodegradation experiments were conducted in triplicate at optimum conditions (or parameters) predicted by the statistical experiments. The time profiles of biomass and substrate concentration were analyzed with a kinetic model (described in subsequent sections).

2.5. Phenanthrene tolerance of *C. tropicalis*:

The tolerance of *C. tropicalis* strain towards phenanthrene was examined with two important factors, viz. (1) biomass growth pattern, and (2) degradation potential of the strain under different initial phenanthrene concentrations in the range 0 – 500 mg L^{-1}. 100 mL BH medium supplemented with phenanthrene (at different initial concentrations) was inoculated with preculture of *C. tropicalis* cells. All experiments were done at optimum conditions obtained from statistical design. A control experiment was done to assess the growth of *C. tropicalis* in BH medium in absence of phenanthrene or any other carbon source. All experiments including the control were conducted for 14 days with three times for the assessment of reproducibility.

2.6. Ultrasound–assisted biodegradation of phenanthrene (test experiments)

Ultrasound–assisted biodegradation of phenanthrene was conducted in an ultrasonic bath (PCi Analytics, India, dimensions – 30 cm × 15 cm × 10 cm, volume – 3.5 L, rated power 100 W, frequency 33 kHz). Before experiments, ultrasonic bath was calibrated with calorimetric technique to determine the ultrasound pressure amplitude and the actual power input. The pressure amplitude

of ultrasonic waves in the medium corresponding to calorimetrically measured acoustic intensity of 0.66 W cm^{-2} was 1.4 bar (or 140 kPa). The water temperature in ultrasound bath was kept at 32° ± 2°C. Moreover, location of the Erlenmeyer flask in the bath was maintained same in every experiment to prevent artifacts due to spatial variation of ultrasound intensity [18].

In biodegradation test experiments, all physical parameters (except mechanical shaking) were at their optimum values, as obtained in validation experiments. Mechanical shaking in control experiments was replaced with a combination of mechanical shaking and sonication at optimum duty cycle. The duty cycle of sonication was also optimized before experiments. Optimum results were obtained for 10% duty cycle, i.e. sonication – 1 min and mechanical shaking – 9 min for every 10 min reaction. Sonication was applied to the broth during log phase of yeast cells (total four days from day 4 to day 8) for 12 h/day @ 10% duty cycle. For the remaining 12 h/day of log phase, the reaction mixture was subjected to mechanical shaking (as done in validation experiments). The experimental protocol of control (mechanical shaking) and test (mechanical shaking + sonication @ 10% duty cycle) experiments is explained in Fig. 1. The duration of all biodegradation experiments was 14 days.

2.7. Analysis of the viability and morphology of yeast cells exposed to sonication

Viability of ultrasound–exposed *C. tropicalis* MTCC 184 cells in test experiments was analyzed by Flow cytometry using a multi–parametric BD FACS Calibur (Becton Dickson, Calibur™ Flow Cytometer, USA). Microbial cells after completion of experiment were examined with 488 nm laser and 530 nm emission filter using propidium iodide (PI). The changes in cell morphology during sonication were assessed on the basis of SSC (Side Scatter) and FSC (Forward Scatter). Side–scattered light (SSC) is proportional to cell complexity or granularity, and forward–scattered light (FSC) is proportional to cell size or surface area.

The *C. tropicalis* cells in both control and test experiments were analysed with FE–SEM (Field Emission Scanning Electron Microscope, Make: Zeiss, Model: Sigma 300) micrographs to

spot any visible differences in morphological and phenotypic characters. Initially, the cells were centrifuged for 10 min at 5,000 rpm, and the resultant pellet was washed thrice with phosphate buffer saline (PBS, pH 7). Further, the pellet was fixed with 2.5% formaldehyde for 1 h and again washed thrice with PBS, followed by a dehydration step using ethanol at different concentration range (10, 30, 50. 70, 90, 100% ethanol) for 30 min. At last, the samples were drop cast on the FE–SEM grid and allowed to dry at 37°C. The grids were coated with gold powder and observed under FE–SEM at magnification of 2.00 KX.

2.8. Chemical oxygen demand (COD) measurement and FTIR analysis

The extent of phenanthrene biodegradation was also assessed in terms of reduction in chemical oxygen demand (COD) and analysis of Fourier Transform Infrared (FTIR) spectra of the samples. Samples from control and test experiments were centrifuged for 5 min at 10,000 rpm, and the aqueous supernatant was taken for COD and FTIR analysis. COD of the samples was quantified using HACH COD reagents and measured in DR900 calorimeter (Hach, USA). The percentage reduction of COD was calculated from initial COD and final COD values.

The absorption bands in the FTIR spectra correspond to the functional groups present in molecular species formed out of phenanthrene biodegradation. The samples were examined after lyophilization (Labconco) using FTIR (Perkin Elmer Spectrum two), and the resulting spectra were matched with FTIR spectrum of pure phenanthrene. The FTIR analysis was done in mid–infrared region from 400 to 4000 cm^{-1}.

3. Kinetic analysis of phenanthrene biodegradation

The previous literature [19] has reported significant substrate inhibition effects during the growth of yeasts, such as *C. tropicalis* on organic pollutants. Substrate (phenanthrene) utilization rate is written as:

$$\frac{dS}{dt} = -qX = -\left(\mu / Y_{x/s}\right) X \tag{2}$$

Notations are as follows: S = phenanthrene concentration (mg L^{-1}), μ = specific biomass (or cell) growth rate (day^{-1}), t = incubation time (day), X = dry cell weight (mg L^{-1}), $Y_{x/s}$ = growth yield coefficient (g g^{-1}), q = specific degradation rate (day^{-1}). Yield factor for biomass, $Y_{x/s}$ (g dry biomass/g phenanthrene) can be calculated as follows:

$$Y_{x/s} = -\frac{dX/dt}{dS/dt} = -\frac{dX}{dS} = -\frac{\left(X - X_0\right)}{\left(S - S_0\right)} \tag{3}$$

Profile of biomass involving growth and decay is written as:

$$\frac{dX}{dt} = \mu X - bX \tag{4}$$

where b = biomass decay coefficient (day^{-1}). For the integration of equations 2 and 4, we have used the value of specific growth rate (μ) corresponding to initial substrate concentration ($S = S_0$). Several kinetic models that account for substrate inhibition are available in the literature. The basic kinetic model for substrate inhibition is Haldane model:

$$\mu = \left.\frac{\mu_{\max} S}{K_S + S + \left(S^2 / K_i\right)}\right|_{S=S_0} \tag{5}$$

where, S = phenanthrene concentration (mg L^{-1}), μ = specific biomass growth rate (day^{-1}), $\mu_{\max}$ = maximum specific biomass growth rate (day^{-1}), K_s = half saturation coefficient (mg L^{-1}), K_i = inhibition coefficient (mg L^{-1}). However, other semi–empirical models reported in the literature are:

Aiba model: $$\mu = \left.\frac{\mu_{\max} S}{K_s + S} \exp\left(-S/K_i\right)\right|_{S=S_0} \tag{6}$$

Edward model: $$\mu = \left.\frac{\mu_{\max} S}{S + K_s + \left(S^2/K_i\right)\left(1 + S/K_s\right)}\right|_{S=S_0} \tag{7}$$

Yano model: $$\mu = \left.\frac{\mu_{\max} S}{S + K_s + \left(S^2/K_i\right)\left(1 + S/K\right)}\right|_{S=S_0} \quad (8)$$

The kinetic parameters in the above models were determined from the analysis of μ and q over a wide range of initial substrate concentrations, viz. S_0 = 25 to 500 mg L^{-1}. The specific biomass growth rate (μ) in the log or exponential phase of each experiment was obtained using basic relation: $dX/dt = -\mu X$ (i.e., equation 4 with decay coefficient assumed as zero), or as slope of the plot $\ln\left(X/X_i\right)$ versus t. The plot of μ versus S_0 was fitted to equations 5 to 8 using non–linear regression method in MATLAB R2018b to yield the growth coefficients $\mu_{\max}$, K, K_S and K_i. The best model for the analysis was selected on the basis of regression coefficient. For determination of specific degradation rate (q), a similar procedure was followed, in which the experimental values of q (specific degradation rate) for varying initial substrate concentrations (S_0) were determined from the degradation profiles for the total 14–day period of experiment. This data was fitted to analogous expressions for q (as a function of S at $S = S_0$), as given in equations 5 to 8, to obtain parameters of $q_{\max}$, K', K'_S, K'_i.

The kinetic parameters of b (decay coefficient) and $Y_{X/S}$ (biomass yield coefficient) in eqs. 2 and 4 were obtained by fitting experimental profiles of biomass and substrate to eqs. 2 and 4 using Genetic Algorithm in MATLAB (R2018b). These equations were simultaneously solved using Runge–Kutta 4th order method (as initial value problem) to obtain the simulated profiles of substrate and biomass. The simulated profiles were compared against the experimental profiles (mean values of biomass and substrate concentrations in the triplicate experimental runs). The sum of RMSE (root mean square error) between the two profiles was minimized by adjusting the numerical values of kinetic parameters in the model within specified bounds [20]. For this purpose, experiments (both control and test) were conducted at optimum conditions obtained from statistical experiments. The initial substrate concentration (corresponding to maximum q and μ) for these experiments was obtained from analysis of substrate inhibition kinetics outlined above.

4. Protein expression and identification of metabolic pathway

The expression and size of crude proteins present in the samples were established by running SDS–PAGE (Sodium dodecyl sulfate polyacrylamide gel electrophoresis). Moreover, phenanthrene degradation pathway by *C. tropicalis* (either *ortho*– or *meta*–cleavage route) under test and control conditions was also identified. The principal enzymes involved in the pathway, viz. catechol 1,2–dioxygenase (C1,2–D) and catechol 2,3–dioxygenase (C2,3–D), are responsible for catechol ring fission through *ortho* or *meta* route. The predominant degradation pathway can be identified by conducting an assay of catechol dioxygenase enzyme activity.

4.1. Protein extraction and expression (SDS–PAGE analysis)

Samples of broth (control and test experiments) were collected and *C. tropicalis* cells were separated by centrifugation at 10,000 rpm for 5 min. The resulting cell pellets were suspended in lysis buffer (5% SDS, 8 M urea, 0.1 mM EDTA, 40 mM Tris–HCl pH 7.5) [21]. Further, the cells were ruptured using a sonicator probe (Sonics & Materials VCX 500) @ 50% duty cycle (30 s on and 30 s off) to extract intracellular proteins. The samples were further centrifuged for 30 min at 10,000 rpm and at 4°C and supernatant were separated. To confirm the expression of proteins, SDS–PAGE (Sodium dodecyl sulfate polyacrylamide gel electrophoresis) analysis was done. 40 µL of the sample was mixed with SDS loading buffer and reducing agent, and then resolved on a 12% SDS–polyacrylamide gel (PAGE). The SDS gel was stained with coomassie brilliant blue dye and was observed in Gel Doc (Bio–RAD, USA) with Image Lab 5.2.1 software. The protein bands were examined according to their respective molecular weights. The total protein content present in samples was estimated by Lowry method with bovine serum albumin (BSA) as standard [22].

4.2. Analysis of enzyme activity

Activities of the two enzymes in the metabolic pathway, C1,2–D, and C2,3–D, were assessed by growing *C. tropicalis* in BHM with phenanthrene as sole carbon source. 7th and 14th–day samples of control and test experiments were used for enzyme activity assay. Catechol dioxygenase activity in the extract was determined according to the standard procedure [23].

4.3. Analysis of catechol 1,2–dioxygenase activity

The catechol 1,2–dioxygenase activity is a signature of the *ortho*–cleavage reaction of catechol leading to *cis,cis*–muconic acid formation. This activity can be quantified using spectrophotometric measurements. The reaction mixture for assessment of C1,2–D activity was added in a quartz cuvette with following composition (total 3 mL): 0.1 mL 2–mercaptoethanol (100 mM), 0.7 mL distilled water, 2 mL Tris–HCl buffer (50 mM, pH 8), 0.1 mL cell–free sample. After thorough mixing, 0.1 mL catechol (0.1 mM) was added. The absorbance of this solution at 260 nm was monitored for 5 min. The rise in absorbance of solution was an indicator of *cis–cis* muconic acid production [24].

4.4. Analysis of catechol 2,3–dioxygenase activity

The presence of catechol 2,3–dioxygenase activity signifies the *meta*–cleavage reaction of catechol with the formation of 2–hydroxymuconic semialdehyde (HMSA). The reaction mixture for assessment of the activity consisted of 0.2 mL cell–free sample, 2 mL Tris–HCl buffer (pH 7.5), and 0.6 mL distilled water. Catechol (100 mM) was added after thorough mixing, and then absorbance was monitored at 375 nm for 5 min. A rise in absorbance essentially signifies formation of HMSA [24].

4.5. Calculation of enzyme activity

The enzymatic activity of one unit (U) can be defined as the quantity of enzyme converting one μmol of the substrate into the product in one minute under specific reaction conditions and can be estimated as:

$$\text{Activity (U mL}^{-1}) = \frac{\Delta E \cdot V_f \cdot 1000}{\Delta t \cdot V_s \cdot L \cdot E_m} \quad (9)$$

where, ΔE = change in absorbance, V_f = final volume, V_s = cell–free extract volume, Δt = time of reaction (5 min), E_m = molar extinction coefficient of the formed product and L = path length (1 cm for standard cuvette). Specific activities of the samples were expressed as units per milligram of protein.

5. Results and Discussion

5.1. Statistical optimization of process parameters

The experimental data obtained from central composite design was fitted to a 2nd–order regression equation as:

$$\begin{aligned} Y = {} & 45.857 - 0.812X_1 + 4.895X_2 + 1.312X_3 + 3.645X_4 - 9.792X_1^2 - 6.354X_2^2 \\ & -0.354X_3^2 - 4.792X_4^2 + 2.406X_1X_2 + 0.031X_1X_3 + 2.343X_1X_4 - 0.218X_2X_3 \\ & -0.656X_2X_4 + 1.593X_3X_4 \end{aligned} \quad (10)$$

The full CCD experimental design, along with the predicted and experimental values of response variable (i.e. percentage degradation) is provided in supplementary material. The global optimum values of variables (process parameters) corresponding to maximum response variable (phenanthrene degradation) were obtained as: medium pH = 6.2, temperature = 33.4°C, agitation speed = 190 rpm and % inoculum = 9.26 vol%. At optimum conditions, the maximum phenanthrene degradation predicted by the quadratic model was 65.19%.

***Validation experiment*:** The substrate and biomass profiles of the validation experiment are given in supplementary material. For 100 mg L^{-1} initial phenanthrene concentration, a residual concentration of 34 ± 2 mg L^{-1} was obtained after 14 days, which corresponded to ~ 66%

degradation. This result matched closely with the predictions of statistical experimental design.

5.2. Tolerance of *C. tropicalis* to phenanthrene

The tolerance of the yeast strain to phenanthrene was studied by performing batch experiments with different initial concentrations of phenanthrene (at optimum conditions predicted by statistical design). The trends of final biomass concentrations and residual phenanthrene concentration are given in supplementary material. The final biomass concentration in the mixture shows a maximum for initial concentration of 100 mg L^{-1} and reduces thereafter. This result demonstrates toxicity of phenanthrene towards the growth of *C. tropicalis* cells. The absolute phenanthrene degradation rises with initial concentration in the mixture, but not proportionately, and this could be a manifestation of inhibition of biomass growth by phenanthrene.

5.3. Kinetic analysis of growth and phenanthrene degradation

The profiles of μ (specific growth rate) and q (specific degradation rate) for different initial concentrations of phenanthrene (S_0) are shown in Fig. 2. These profiles were fitted to various substrate inhibition models using nonlinear regression method (MATLAB R2018b). The kinetic parameters in various models obtained after fitting the profiles are listed in Table 3. The Haldane model had the best fit for profiles of both μ and q with the highest R^2 and the lowest RMSE. The kinetic parameters for Haldane model for biomass growth were: μ_{max} = 0.6 day^{-1}, K_s = 27.54 mg L^{-1}, K_i = 428.4 mg L^{-1}. The corresponding parameters for degradation profile were: q_{max} = 0.18 day^{-1}, K'_s = 46.89 mg L^{-1}, K'_i = 117.5 mg L^{-1}. The profiles of μ and q in Fig. 2 show maxima at S_0 = 100 mg L^{-1}. Reduction in μ and q after S_0 = 100 mg L^{-1} is an indication of substrate inhibition at relatively higher concentrations of phenanthrene. Moreover, relatively faster reduction in q with initial substrate concentration after S_0 = 100 mg L^{-1} indicates greater influence of substrate inhibition on phenanthrene degradation than biomass growth. This is also reflected in terms of ~4×

higher value of K_i (inhibition constant for biomass growth) than K_i' (inhibition constant for substrate degradation).

5.4. Phenanthrene degradation: control and test experiments

The results of phenanthrene degradation under control (mechanical shaking), and test (combination of sonication @ 10% duty cycle and mechanical shaking) conditions are shown in Fig. 3. The experimental time profiles of concentrations (substrate and biomass) were fitted to equations 2 and 4 using numerical solutions coupled with Genetic algorithm. The simulated time profiles of biomass and substrate are also shown in Fig. 3. The regressions coefficients R^2 for all profiles are > 0.9, indicating good match between simulations and experimental profiles. The final results of both experiments (control and test) are tabulated in Table 4, which depicts the kinetic parameters (b and $Y_{X/S}$) in eqs. 2 and 4, along with total absolute phenanthrene degradation. The phenanthrene degradation shows ~ 25% rise under test conditions. The biomass yield coefficient ($Y_{X/S}$) also shows 25% rise in test experiments, while the decay coefficient (b) reduces ~ 21%. Enhanced phenanthrene degradation with higher cell growth in test experiments can be attributed to several beneficial effects of sonication on reaction system as follows:

(1) intense microturbulence generated by sonication enhances the cell membrane permeability, which facilitates quicker cellular transport of nutrients, substrate, and other metabolites [25], [26].

(2) microturbulence also causes deagglomeration of cell clusters, which helps better access to nutrients and substrate in broth [27].

(3) microturbulence also causes dilution of toxic substances produced during substrate utilization, which helps in reducing cell death and enhancing cell growth.

In the present study, we have attempted to explore an additional facet of protein overexpression induced by sonication that could influence intracellular metabolism, as explained in subsequent section.

5.5. Viability and morphological changes in yeast cells exposed to sonication

Fig. 4 demonstrates the results of flow cytometry study for assessing the viability of *C. tropicalis* cells after exposure to ultrasound. Live and dead yeast cells were characterized by their distinct staining characteristics with PI stain. No substantial alteration occurred in FSC and SSC of the cells after sonication, as shown in Figs. 4 A and B, which implied that the cell morphology and internal complexity of *C. tropicalis* remained practically unchanged after sonication. The percentage of live cells present in control and test experiments was determined from the acquisition dot plots between FSC and FL3 given in Figs. 4 C and D. The percentage of live cells in both test (82.80%) and control (84.93%) experiments did not differ much. In concurrence, the histograms of PI + cells in Figs. 4 E and F show a similar percentage of dead cells in control (14.93%) and test (17.04%) experiments. These results clearly demonstrate no adverse effect of sonication on microbial cells.

The FESEM micrographs of *C. tropicalis* cells are shown in Figs. 5A and B. A comparison of these micrographs does not show any significant difference in morphology and topography of the cells. The micrographs for test experiment also do not show any visible cell damage, rupture, or debris, indicating that the cells remained intact during exposure to sonication. Thus, the results of FESEM analysis were in concurrence with the results of flow cytometry.

5.6. COD removal and FTIR analysis

Chemical oxygen demand (COD) was used as an indicative measure of residual organic matter. The reduction in COD in control and test experiments was monitored. It was observed that 60% COD removal was achieved in control experiments, while 69% COD removal was achieved in test experiments. Relatively higher reduction in COD is attributed to enhancement of phenanthrene biodegradation by sonication. Moreover, only 3 – 5 % of COD was degraded in the abiotic samples. Another probable cause of higher COD removal by sonication is formation of water–soluble products due to reaction between phenanthrene and $^{\bullet}OH$ radicals generated by

sonication. Greater details of COD analysis are given supplementary material.

FTIR analysis was used to identify the functional groups of the species present in samples of both experiments (control and test), which are indicative of phenanthrene degradation. The IR spectra of the samples are shown in Fig. 6. In Fig. 6 A, the band between 2800 – 3200 cm^{-1} (3054 cm^{-1}) is resultant of proton (H) stretching and indicates aromatic C-H band stretching in pure phenanthrene [28]. Similarly, bands between 1200 – 1600 cm^{-1} (1451 cm^{-1}, 1454 cm^{-1}, 1498 cm^{-1}) denote the skeleton vibration peaks of benzene ring in pure phenanthrene. Moreover, band at 729 cm^{-1} signify four binding proton connected to benzene ring and the band at 815 cm^{-1} denotes a further proton bond to benzene ring. The spectrum of final sample (drawn at the end of experiment) is different from the spectrum of pure phenanthrene, as it contains several intermediate species formed during biodegradation of phenanthrene. In control and test experiments (Fig 6 B and C), intense peaks were observed at 3262 cm^{-1} and 3257 cm^{-1}, respectively, signifying free O-H stretching vibrations, while strong bands at 1595 cm^{-1} and 1634cm^{-1} correspond to aromatic C–C stretching and NH_2 bending vibration. The peaks within 1039 – 1400 cm^{-1} range corresponds to CH_3, CH_2 bending deformation, and C–N stretching, while peaks in the range of 800 cm^{-1} and 500 cm^{-1} indicate C–H bend and C–Br stretch, respectively. The FTIR results thus confirm degradation of phenanthrene with formation of different metabolites having different functional groups. It is noteworthy that FTIR spectra of final samples from both experiments (control and test) comprise of peaks in the same range, indicating formation of same metabolites (or in other words same degradation pathway). This also indicates that sonication only enhances the kinetics of metabolic reactions but does not alter the metabolic pathway.

As seen from Table 1, the phenanthrene degradation (84% in 14 days) as well as COD removal (69%) in the present work was higher than previous studies employing fungi and yeast (or specifically the *Candida* sp.). Moreover, a peculiar facet of the present study, as compared to the previous literature, is that phenanthrene has been used as sole carbon source with no

supplementation of other carbon source or additives.

5.7. SDS–PAGE analysis of protein expressions

The intracellular proteins in the samples from control and test experiments were extracted and resolved on a 12% SDS–polyacrylamide gel (PAGE) by electrophoresis and stained with coomassie brilliant blue. The protein ladder marker used in the experiment was protein molecular weight marker (Low) (97.2 kDa to 14.3 kDa) (Company: Takara, Code no:3450) [29]. Fig. 7 shows the gel image of SDS–PAGE analysis of protein expression in control and test experiments. Comparing the protein bands in lane 1 (test) and lane 2 (control) reveals much higher expression of the proteins in test experiments. This is clear evidence of enhanced metabolism that results in faster degradation of phenanthrene.

Bands of different sizes were visible in the lanes of both control and test samples. Among various proteins that facilitate phenanthrene degradation, catechol 2,3–dioxygenase (C2,3–D), possessing a size of 35.0 kDa [30], is a key enzyme in the *meta*–route of degradation (refer to Fig. 8 depicting the metabolic pathway of phenanthrene degradation). SDS–PAGE analysis of both test and control samples revealed that it contained a protein band (Fig. 7), whose size was in good agreement with that of C2,3–D (35.0 kDa). Moreover, this band was more expressed in test samples (lane 1), indicating higher production of this protein under the influence of sonication [31].

5.8. Identification of metabolic pathway

Biodegradation of phenanthrene, as depicted in Fig. 8, is known to occur via catechol degradation pathway. Catechol is a common intermediate in polycyclic aromatic biodegradation [24], [32]. It is further degraded through *ortho*– or *meta*– cleavage route, as displayed in Fig. 8. As noted earlier, the *ortho*–cleavage route leads to *cis,cis*–muconic acid, whereas the *meta* route results in HMSA formation. Contributions of both *meta* and *ortho* pathways can be discerned by quantification of the characteristic enzymes, C2,3–D for *meta* pathway, and C1,2–D for *ortho*

pathway [23], [33]. To identify the impact of sonication on catechol ring cleavage route, enzymatic assay for C1,2–D and C2,3–D was carried out on 7th and 14th day of degradation in both control and test experiments. There was no rise in absorbance at 260 nm during C1,2–D assay in control and test experiments, i.e. no C1,2–D activity and no *cis,cis*–muconic acid production. During C2,3–D assay for 7th and 14th day of degradation, rise in absorbance at 375 nm was observed in both control and test experiments signifying strong activity of C2,3–D enzyme. Absorbance profiles of C2,3–D enzyme in control and test experiments are given in supplementary material. The absorbance values for test experiments were higher than control for both days, which indicates greater enzyme production and faster metabolism in test experiments.

5.9. Catechol 2, 3–dioxygenase enzyme activity

The activities (U mL^{-1}) and the specific activities (mol min^{-1} mg^{-1}) of the C2,3–D enzyme are given in Table 5. The activities were determined on the 7th and 14th day of the experiment. 2–hydroxymuconic semialdehyde (HMSA) possessed molar extinction coefficient of 36,000 M^{-1} cm^{-1} [34]. C2,3–D activity in samples of test experiments on both 7th and 14th day was higher than the corresponding samples of control experiments. Moreover, specific activity of C2,3–D enzyme in control and test experiments decreased with time. A possible reason underlying this effect could be inhibition induced by intermediate metabolites of phenanthrene degradation. On relative basis, the reduction in specific activities of the enzymes was higher in control experiments for both 7th and 14th day of degradation. This essentially points to relatively lesser inhibition and inactivation of the cellular enzymes in test experiments. A plausible cause underlying this effect could be enhanced cellular transport induced by microturbulence generated during sonication. Another possible cause leading to higher activity of enzymes in test experiments, as demonstrated in previous literature [35] is alterations in secondary structure of enzyme produced due to sonication. These alterations include reduction in the rigid α–helix content leading to unfolding of proteins that exposes inner

hydrophobic group and substrate–binding sites. These changes in secondary structure leads to faster metabolism.

These results clearly show that the enhancement effect of sonication on phenanthrene biodegradation is mainly of physical nature. The metabolic pathway of degradation is not influenced by sonication, as phenanthrene degraded through *meta*– cleavage pathway in both control and test experiments.

6. Conclusion

A mechanistic analysis of sonication–induced enhancement of phenanthrene removal using *C. tropicalis* cells has revealed several interesting facets of the bioremediation process. To begin with, optimum physical parameters for degradation were obtained through the statistical design of experiments. The enhancement effect of sonication was assessed by replacing mechanical shaking with sonication (@ 10% duty cycle) during log phase. A 25% rise in phenanthrene degradation was seen. Analysis of kinetics of degradation revealed strong substrate inhibition for initial concentrations > 100 mg L^{-1}. The biomass yield coefficient increased while the decay coefficient of the cells reduced in presence of sonication. SDS–PAGE analysis of intracellular protein expression showed overexpression of total proteins in presence of sonication. Proteins overexpressed during sonication revealed a band of 35.0 kDa size, which can be predicted as catechol 2,3–dioxygenase (C2,3–D), an important enzyme involved in phenanthrene degradation through *meta*–cleavage route. Activity of C2,3–D enzyme was found to be higher in sonicated samples, which resulted in higher degradation. A probable cause underlying these effects is enhanced permeability of cell membranes in presence of sonication that promotes cellular transport of nutrients, substrate, and metabolites. Finally, flow cytometry analysis showed no adverse effect of ultrasound on cell viability and morphology. The present study also forms useful basis for further in–depth investigation on influence of sonication on intracellular proteins and cell metabolism of *Candida tropicalis*.

Acknowledgments

Authors would like to acknowledge infrastructure support provided by Central Instrumentation facility of I.I.T. Guwahati. Authors also acknowledge Dept. of Biosciences and Bioengineering, I.I.T. Guwahati for Flow Cytometry analysis.

Conflicts of interest

Authors declare no conflicts of interest of any kind.

Appendix A: Supplementary data

Supplementary data to this article can be found in the online version of the article.

References

[1] T.C. Feng, C.Z. Cui, F. Dong, Y.Y. Feng, Y.D. Liu, X.M. Yang, Phenanthrene biodegradation by halophilic *Martelella sp*. AD–3, J. Appl. Microbiol. 113 (2012) 779 – 789.

[2] A. Chebbi, D. Hentati, H. Zaghden, N. Baccar, F. Rezgui, M. Chalbi, S. Sayadi, M. Chamkha, Polycyclic aromatic hydrocarbon degradation and biosurfactant production by a newly isolated *Pseudomonas* sp. strain from used motor oil-contaminated soil, Int. Biodeter. Biodegr. 122 (2017) 128 – 140.

[3] D.H.Y. Yanto, N.P.R.A. Krishanti, F.C. Ardiati, S.H. Anita, I.K. Nugraha, F.P. Sari, R.P.B. Laksana, S. Sapardi, T. Watanabe, Biodegradation of styrofoam waste by ligninolytic fungi and bacteria, IOP Conf. Series: Earth and Environmental Science 308 (2019) 012001.

[4] A. Hidayat, D.H.Y. Yanto, Biodegradation and metabolic pathway of phenanthrene by a new tropical fungus, *Trametes hirsuta* D7, J. Environ. Chem. Eng. 6 (2018) 2454 – 2460.

[5] S.H. Anita, F.P. Sari, D.H.Y. Yanto, Decolorization of Synthetic Dyes by Ligninolytic Enzymes from *Trametes hirsuta* D7, Makara J. Sci. (2019) 44 – 50.

[6] D.H.Y. Yanto, S. Tachibana, Potential of fungal co-culturing for accelerated biodegradation of petroleum hydrocarbons in soil, J. Hazard. Mater. 278 (2014) 454 – 463.

[7] M. Marco–Urrea, I. Garcia–Romera, E. Aranda, Potential of non–ligninolytic fungi in bioremediation of chlorinated and polycyclic aromatic hydrocarbons, New Biotechnol. 32 (2015) 620 – 628.

[8] F. Pan, Q. Yang, Y. Zhang, S. Zhang, M. Yang, Biodegradation of polycyclic aromatic hydrocarbons by *Pichia anomala*, Biotechnol. Lett. 26 (2004) 803 – 806.

[9] A.E.L. Hesham, Z. Wang, Y. Zhang, J. Zhang, W. Lv, M. Yang, Isolation and identification of a yeast strain capable of degrading four and five ring aromatic hydrocarbons, Ann. Microbiol. 56 (2006) 109 – 112.

[10] A. Reyes–Cesar, A.E. Absalon, F.J. Fernandez, J.M. Gonzalez, D.V. Cortes–Espinosa, Biodegradation of a mixture of PAHs by non–ligninolytic fungal strains isolated from crude oil–contaminated soil, World J. Microbiol. Biotechnol. 30 (2014) 999 – 1009.

[11] F. Deeba, V. Pruthi, Y.S. Negi, Aromatic hydrocarbon biodegradation activates neutral lipid biosynthesis in oleaginous yeast, Bioresour. Technol. 255 (2018) 273 – 280.

[12] O. Csutak, I. Stoica, R. Ghindea, A.M. Tanase, T. Vassu, Insights on yeast bioremediation processes, Roman. Biotechnol. Lett. 15 (2010) 5066 – 5071.

[13] Z.D. Umar, N.A.A. Aziz, Z.S. Zulkifli, M. Mustafa, Rapid biodegradation of polycyclic aromatic hydrocarbons (PAHs) using effective *Cronobacter sakazakii* MM045 (KT933253), MethodsX 4 (2017) 104 – 117.

[14] N. Hou, N. Zhang, T. Jia, Y. Sun, Y. Dai, Q. Wang, D. Li, Z. Luo, C. Li, Biodegradation of phenanthrene by biodemulsifier–producing strain *Achromobacter* sp. LH–1 and the study on its metabolisms and fermentation kinetics, Ecotoxicol. Environ. Saf. 163 (2018) 205 – 214.

[15] J.B. Bhasarkar, P. Dikshit, V.S. Moholkar, Ultrasound Assisted Biodesulfurization of Liquid Fuel using Free and Immobilized Cells of *Rhodococcus rhodochrous* MTCC 3552: A

Mechanistic Investigation, Bioresour. Technol. 187 (2015) 369 – 378.

[16] M.H. Khorasanizadeh, R. Monsef, O. Amiri, M. Amiri, M. Salavati-Niasari, Sonochemical-assisted route for synthesis of spherical shaped holmium vanadate nanocatalyst for polluted waste water treatment, Ultrason. Sonochem. 58 (2019) 104686.

[17] R. Monsef, M. Ghiyasiyan-Arani, M. Salavati-Niasari, Application of ultrasound-aided method for the synthesis of NdVO4 nano-photocatalyst and investigation of eliminate dye in contaminant water, Ultrason. Sonochem. 42 (2018) 201 – 211.

[18] V.S. Moholkar, S.P. Sable, A.B. Pandit, Mapping the cavitation intensity in an ultrasonic bath using the acoustic emission, AIChE J. 46 (2002) 684 – 694.

[19] B. Basak, B. Bhunia, S. Dutta, S. Chakraborty, A. Dey, Kinetics of phenol biodegradation at high concentration by a metabolically versatile isolated yeast *Candida tropicalis* PHB5, Environ. Sci. Pollut. Res. 21 (2014) 1444 – 1454.

[20] B. Z. Tizazu, K. Roy, V. S. Moholkar, Mechanistic investigations in ultrasound–assisted xylitol fermentation, Ultrason. Sonochem. 48 (2018) 321 – 328.

[21] K.K. Datta, A.H. Patil, K. Patel, G. Dey, A.K. Madugundu, S. Renuse, J.E. Kaviyil, R. Sekhar, A. Arunima, B. Daswani, I. Kaur, Proteogenomics of *Candida tropicalis*—An opportunistic pathogen with importance for global health, Omics: a journal of integrative biology 20 (2016) 239 – 247.

[22] O.H. Lowry, N.J. Rosebrough, A.L. Farr, R.J. Randall, Protein measurement with the Folin phenol reagent, J. Biol. Chem. 193 (1951) 265 – 275.

[23] M. Mahiudddin, A.M.N. Fakhruddin, A. Al–Mahin, Degradation of phenol via meta cleavage pathway by *Pseudomonas fluorescens* PU1, Int. Scholarly Res. Not. ISRN Microbiol. 2012 (2012).

[24] G.R. Shetty, V.K. Shetty, Pathway identification, enzyme activity and kinetic study for the biodegradation of phenol by *Nocardia hydrocarbonoxydans* NCIM 2386, Desalin. Water Treat. 57 (2016) 8789 – 8801.

[25] F. Chemat, M.K. Khan, Applications of ultrasound in food technology: processing, preservation and extraction, Ultrason. Sonochem. 18 (2011) 813– 835.

[26] G. Huang, S. Chen, C. Dai, L. Sun, W. Sun, Y. Tang, F. Xiong, R. He, H. Ma, Effects of ultrasound on microbial growth and enzyme activity, Ultrason. Sonochem. 37 (2017a) 144 – 149.

[27] D.N. Avhad, V.K. Rathod, Ultrasound assisted production of a fibrinolytic enzyme in a bioreactor, Ultrason. Sonochem. 22 (2015) 257 – 264.

[28] M.L. Wu, M.Q. Nie, X.C. Wang, J.M. Su, W. Cao, Analysis of phenanthrene biodegradation by using FTIR, UV and GC–MS, Spectrochim. Acta. A Mol. Biomol. Spectrosc. 75 (2010) 1047 – 1050.

[29] K. Verma, G. Saha, L.M. Kundu, V.K. Dubey, Biochemical characterization of a stable azoreductase enzyme from *Chromobacterium violaceum*: Application in industrial effluent dye degradation, Int. J. Biol. Macromol. 121 (2019) 1011 – 1018.

[30] M. Takeo, M. Nishimura, M. Shirai, H. Takahashi, S. Negoro, Purification and characterization of catechol 2, 3–dioxygenase from the aniline degradation pathway of *Acinetobacter* sp. YAA and its mutant enzyme, which resists substrate inhibition, Biosci. Biotechnol. Biochem. 71 (2007) 1688 – 1675.

[31] G. Huang, Y. Tang, L. Sun, H. Xing, H. Ma, R. He, Ultrasonic irradiation of low intensity with a mode of sweeping frequency enhances the membrane permeability and cell growth rate of *Candida tropicalis*, Ultrason. Sonochem. 37 (2017b) 518 – 528.

[32] L. Salam, M. Ilori, O. Amund, Pyrene Biodegradation Potential of an Actinomycete, *Microbacterium Esteraromaticum* isolated from Tropical Hydrocarbon–Contaminated Soil, J. Microbiol. Biotech. Food. Sci. 6 (2017) 995 – 1000

[33] A. Banerjee, A.K. Ghoshal, Phenol degradation by *Bacillus cereus*: pathway and kinetic modeling, Bioresour. Technol. 101 (2010) 5501 – 5507.

[34] H. Arai, T. Ohishi, M.Y. Chang, T. Kudo, Arrangement and regulation of the genes for meta–pathway enzymes required for degradation of phenol in *Comamonas testosteroni* TA441, Microbiol. 146 (2000) 1707 – 1715.

[35] M. Agarwal, P.K. Dikshit, J.B. Bhasarkar, A.J. Borah, V.S. Moholkar, Physical insight into ultrasound–assisted biodesulfurization using free and immobilized cells of *Rhodococcus rhodochrous* MTCC 3552, Chem. Eng. J. 295 (2016) 254 – 267.

[36] A.E. Hesham, S.A. Alamri, S. Khan, M.E. Mahmoud, H.M. Mahmoud, Isolation and molecular genetic characterization of a yeast strain able to degrade petroleum polycyclic aromatic hydrocarbons, African J. Biotechnol. 8 (2009) 2218 – 2223.

[37] T. Hadibarata, S. Tachibana, Characterization of phenanthrene degradation by strain *Polyporus* sp. S133, J. Environ. Sci. 22 (2010) 142 – 149.

[38] F. Acevedo, L. Pizzul, M. del Pilar Castillo, R. Cuevas, M.C. Diez, Degradation of polycyclic aromatic hydrocarbons by the Chilean white-rot fungus *Anthracophyllum discolor*, J. Hazard. Mater. 185 (2011) 212 – 219.

[39] S. Farag, N.A. Soliman, Biodegradation of crude petroleum oil and environmental pollutants by *Candida tropicalis* strain, Brazilian Archi. Biol. Technol. 54 (2011) 821 – 830.

[40] X.K. Ma, L. ling Wu, H. Fam, Heavy metal ions affecting the removal of polycyclic aromatic hydrocarbons by fungi with heavy-metal resistance, Appl. Microbiol. Biot. 98 (2014) 9817 – 9827.

[41] M. Lin, X. Hu, W. Chen, H. Wang, C. Wang, Biodegradation of phenanthrene by *Pseudomonas* sp. BZ-3, isolated from crude oil contaminated soil, Int. Biodeter. Biodegrad. 94 (2014) 176 – 181.

[42] H. Wang, J. Lou, H. Gu, X. Luo, L. Yang, L. Wu, Y. Liu, J. Wu, J. Xu, Efficient biodegradation of phenanthrene by a novel strain *Massilia* sp. WF1 isolated from a PAH-contaminated soil, Environ. Sci. Pollut. Res. 23 (2016) 13378 – 13388.

[43] P. Singh, B.N. Tiwary, Optimization of conditions for polycyclic aromatic hydrocarbons (PAHs) degradation by *Pseudomonas stutzeri* P2 isolated from Chirimiri coal mines, Biocatal. Agric. Biotechnol. 10 (2017) 20 – 29.

[44] J.B.S. Haldane, Enzyme. MIT Press, Cambridge, MA. 1965.

[45] S. Aiba, M. Shoda, M. Nagalani, Kinetics of product inhibition in alcohol fermentation, Biotechnol. Bioeng. 10 (1968) 845 – 864.

[46] V.H. Edwards, The influence of high substrate concentrations on microbial kinetics, Biotechnol. Bioeng. 12 (1970) 679 – 712.

[47] T. Yano, T. Nakahara, S. Kamiyama, K. Yamada, Kinetic studies on microbial activities in concentrated solutions. Effect of excess sugars on oxygen uptake rate of a cell–free respiratory system, Agric. Biol. Chem. 30 (1966) 42 – 48.

Table 1: Summary of literature on polycyclic aromatic hydrocarbon degradation using different microbial strains

Microbial Strain	PAH degraded	Carbon source	Degradation medium	Initial conc.	Process parameters	Degradation	Reference
Pichia anomala	Phenanthrene	Phenanthrene	Basal medium (BM)	5.04 mg/L	pH = 5.0-6.0 Temperature = 27°C Agitation = 150 rpm Time = 10 days	5.04 mg/L	[9]
Candida viswanathii	Naphthalene Phenanthrene Pyrene Benzo(a)pyrene	Naphthalene Phenanthrene Pyrene Benzo(a)pyrene + 50g Tween 80	Basal medium (BM) + 0.5g yeast extract + 10g glucose	1.79 mg/kg 1.89 mg/kg 1.96 mg/kg 1.98 mg/kg	pH = 5.0-6.0 Temperature = 27°C Agitation = 150 rpm Time = 10 days	89.76% 77.21% 60.77% 55.53%	[36]
Polyporus sp. S133	Phenanthrene	Phenanthrene + Tween 80	Mineral salt broth (MSB)	1 mmol/L	Temperature = 25°C Agitation = 120 rpm Time = 30 days	92.00%	[37]
Anthracophyllum discolor	Anthracene Phenanthrene Fluoranthene Pyrene	Anthracene Phenanthrene Fluoranthene Pyrene	Kirk medium + Tween 80 (0.05% v/v)	50 mg/L	pH = 6.6 Temperature = 30°C Time = 28 days	22.60 % 7.00 % 19.50 % 8.50 %	[38]
Candida tropicalis	Naphthalene Phenenthrene	Naphthalene Phenenthrene	Natural salt water (NSW) + 0.5% glucose + 0.5% yeast extract	500 mg/L	pH = 7.0 Temperature = 30°C Agitation = 200 rpm Time = 3 days	97.85% 22.00%	[39]
Acremonium sp. P0997	Naphthalene, Fluorene Phenanthrene, Anthracene Fluoranthene	Naphthalene, Fluorene Phenanthrene, Anthracene Fluoranthene	Mineral medium	25 mg/L	pH = 6.5 Temperature = 28°C Agitation = 160 rpm Time = 15 days	96.90 % 71.80 % 67.00 % 85.00 % 87.90 %	[40]
Pseudomonas sp. BZ-3	Phenanthrene	Phenanthrene	Mineral salt medium (MSM) + 20g/L salinity	50 mg/L	pH = 7.0 Temperature = 30°C Agitation = 180 rpm Time = 7 days	75 %	[41]

Table 1 (*continued*)……

Microbial Strain	**PAH degraded**	**Carbon source**	**Degradation medium**	**Initial conc.**	**Process parameters**	**Degradation**	**Reference**
Massilia sp. WF1	Phenanthrene	Phenanthrene	Mineral salt medium (MSM)	100 mg/L	pH = 6.0 Temperature = 28°C Agitation = 130 rpm Time = 2 days	100 mg/L	[42]
Pseudomonas sp. W10	Phenanthrene	Phenanthrene	Basal medium (BM)	200 mg/L	pH = 8.0 Temperature = 37°C Agitation = 180 rpm Time = 30 days	80.00 %	[2]
Pseudomonas stutzeri P2	Phenanthrene Pyrene	Phenanthrene Pyrene	Carbon-free mineral medium (CFMM)	1000 mg/L 500 mg/L	pH = 7.0 Temperature = 30°C Agitation = 150 rpm Time = 7 & 10 days	98.00 % 92.60 %	[43]
Achromobacter sp. LH1	Phenanthrene	Phenanthrene	Mineral salt medium (MSM)	100 mg/L	Temperature = 30°C Agitation = 150 g Time = 7 days	94.00%	[14]
Trametes hirsuta D7	Phenanthrene	Phenanthrene + 1% Tween 80	Mineral salt broth (MSB)	0.056 mM	Temperature = 25°C Time = 15 days	71.73%	[4]
***Candida tropicalis* MTCC 184**	**Phenanthrene**	**Phenanthrene**	**Bushnell-Haas (BH) medium**	**100 mg/L**	**pH = 6.2 Temperature = 33.4°C Agitation = 190 rpm**	**67.00 % (Shaking) 84.00* % (Sonication)**	**(Present work)**

Table 2. Factors and levels of central composite experimental design (actual and coded values)

Factors	Levels	
	Low (–1)	High (+1)
Medium pH (X_1)	4	8
Temperature (°C) (X_2)	20	40
Mechanical shaking (rpm) (X_3)	130	170
Inoculum size (%, v/v) (X_4)	5	10

Table 3. Predicted kinetic parameters of phenanthrene biodegradation by *C. tropicalis* acquired from different models

Mathematical model		Parameters for μ						Parameters for q					
		μ_{max}	K_s	K_i	K	R^2	*RMSE*	q_{max}	K_s'	K_i'	K'	R^2	*RMSE*
Haldane [44]	$\mu = \left.\frac{\mu_{max} S}{K_s + S + \left(S^2 / K_i\right)}\right\|_{S=S_0}$	0.60	27.54	428.4	–	0.98	0.0082	0.18	46.89	117.5	–	0.98	0.0039
Aiba [45]	$\mu = \left.\frac{\mu_{max} S}{K_s + S} \exp\left(-S/K_i\right)\right\|_{S=S_0}$	0.49	21.00	1045.0	–	0.83	0.0275	0.16	52.00	293.5	–	0.90	0.0089
Edward [46]	$\mu = \left.\frac{\mu_{max} S}{S + K_s + \left(S^2/K_i\right)\left(1 + S/K_s\right)}\right\|_{S=S_0}$	0.55	31.47	6458.0	–	0.73	0.0349	0.16	71.00	659.3	–	0.83	0.0107
Yano [47]	$\mu = \left.\frac{\mu_{max} S}{S + K_s + \left(S^2/K_i\right)\left(1 + S/K\right)}\right\|_{S=S_0}$	0.71	50.00	449.0	786.0	0.74	0.0342	0.22	74.48	98.04	1817.0	0.95	0.0068

Notations are as follows: S = phenanthrene concentration (mg L^{-1}), μ = specific biomass (or cell) growth rate (day^{-1}), μ_{max} = maximum specific biomass (or cell) growth rate (day^{-1}), q = specific degradation rate (day^{-1}), q_{max} = maximum specific degradation rate (day^{-1}). K_s, K_i, K = half saturation coefficient, inhibition coefficient, constant respectively, applied to growth rate (mg L^{-1}), K_s', K_i', K' = half saturation coefficient, inhibition coefficient, constant respectively, applied to specific degradation rate (mg L^{-1}).

Table 4. Kinetic parameters for biomass and substrate concentration profiles

Initial substrate concentration (mg L^{-1})	b (day^{-1})	$Y_{X/S}$ (g g^{-1})	S_d (mg)
100 (Control)	0.087	0.004	6.7 ± 0.36
100 (Test)	0.069	0.005	8.4 ± 0.42

Note: S_d is actual amount of pollutant degraded: $(S_0 - S_f) \times V$ (S_0 – initial concentration, S_f – final concentration, V – volume of the reaction mixture)

Table 5. Catechol 2,3–dioxygenase activity of the control and test experiments

Sample	Activity (U mL^{-1})	Protein concentration (mg mL^{-1})	Specific activity (mol min^{-1} mg^{-1})
Control (7^{th} day)	0.00475	28.90×10^{-4}	1.64×10^{-6}
Control (14^{th} day)	0.00612	47.51×10^{-4}	1.28×10^{-6}
Test (7^{th} day)	0.00520	30.76×10^{-4}	1.69×10^{-6}
Test (14^{th} day)	0.00693	51.83×10^{-4}	1.34×10^{-6}

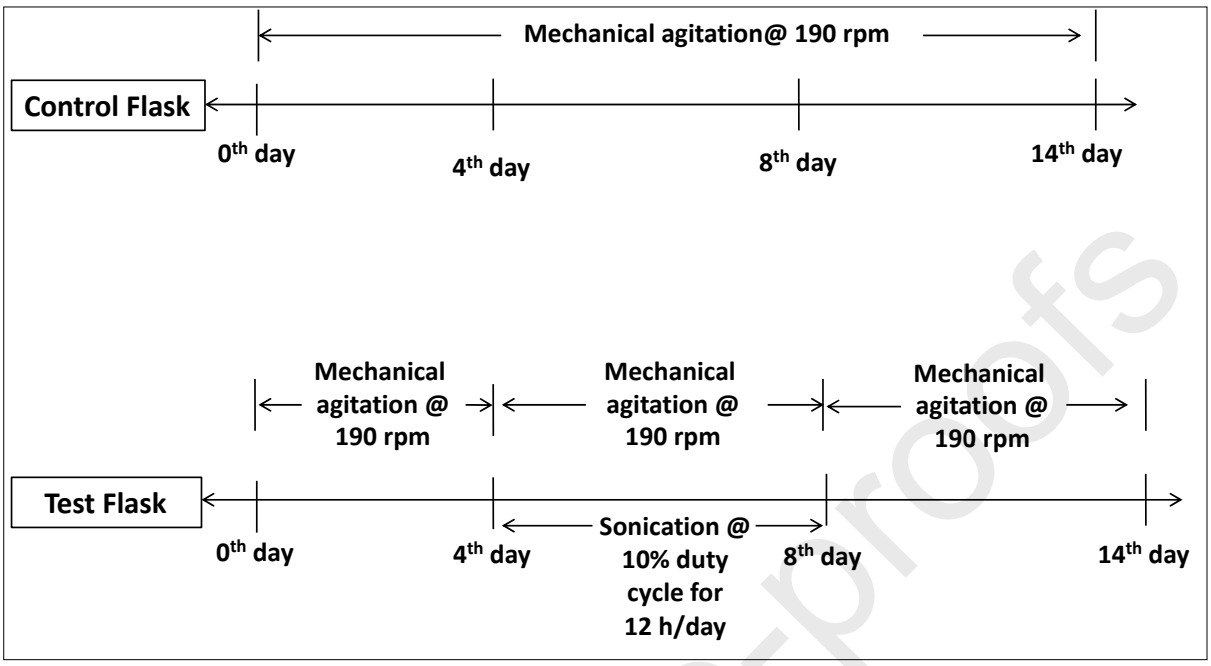

Figure 1. Schematic of the experimental protocol for control and test experiments.

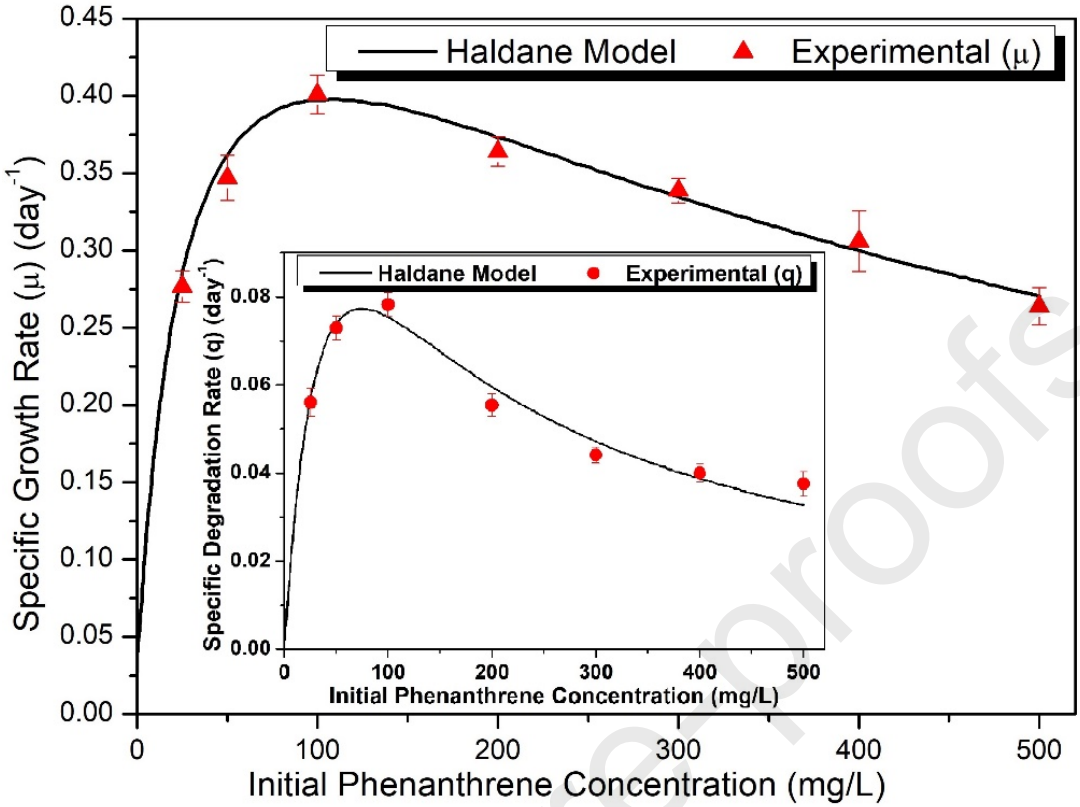

(A)

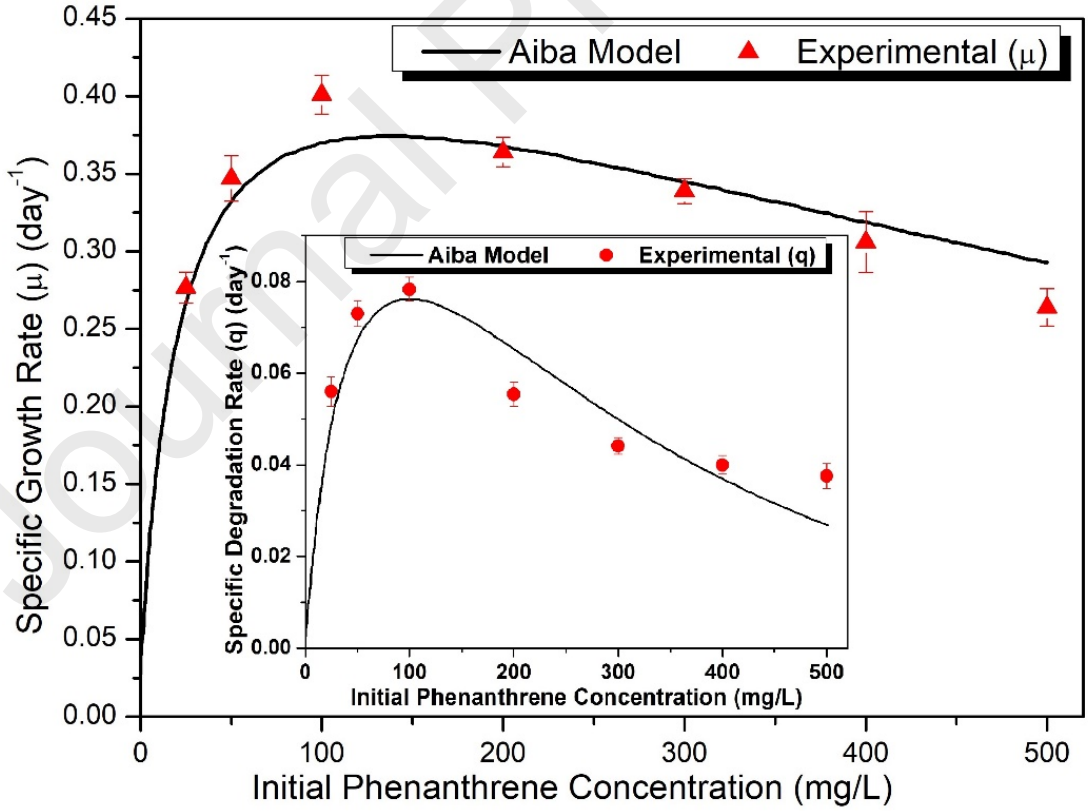

(B)

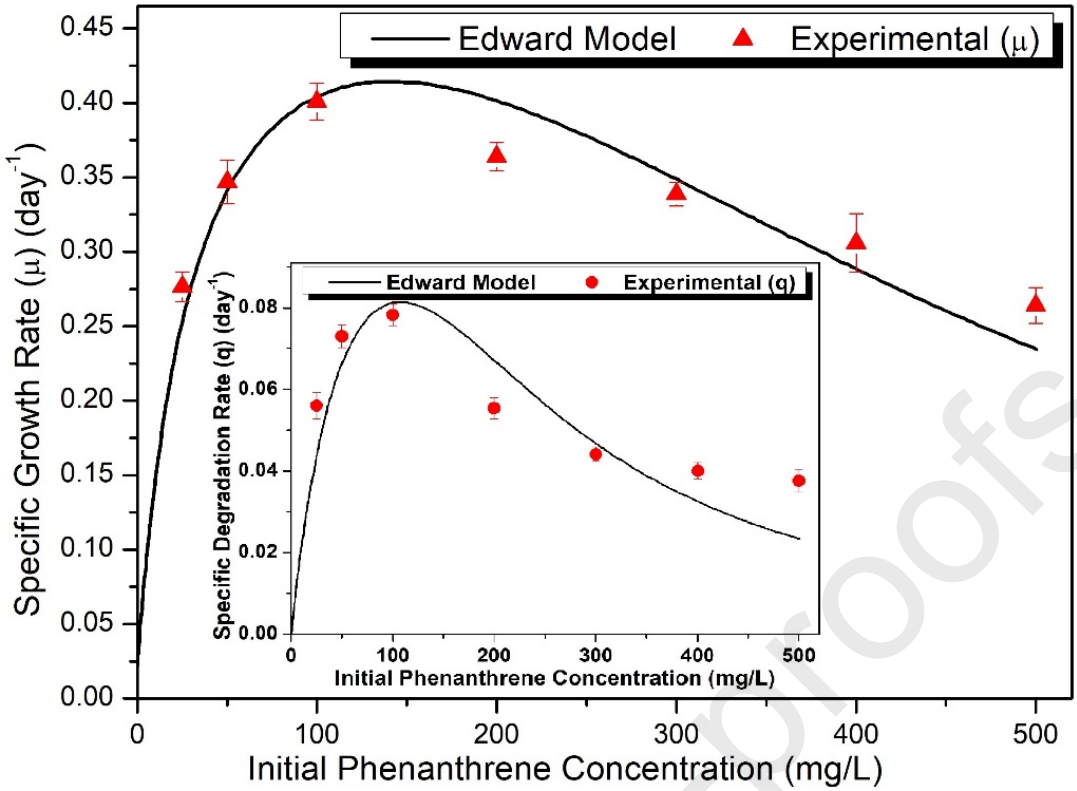

(C)

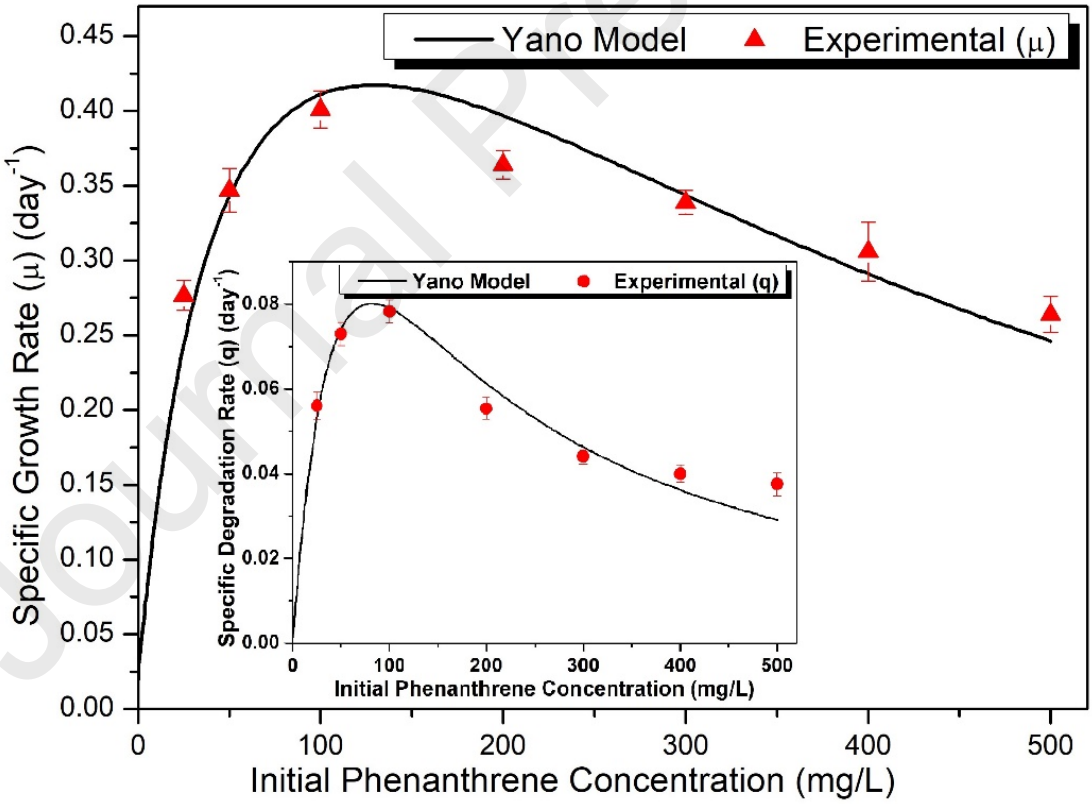

(D)

Figure 2. Experimental and predicted specific growth rate (μ) and substrate degradation rate (q) obtained from different models (A) Haldane model, (B) Aiba model, (C) Edward model, (D) Yano model.

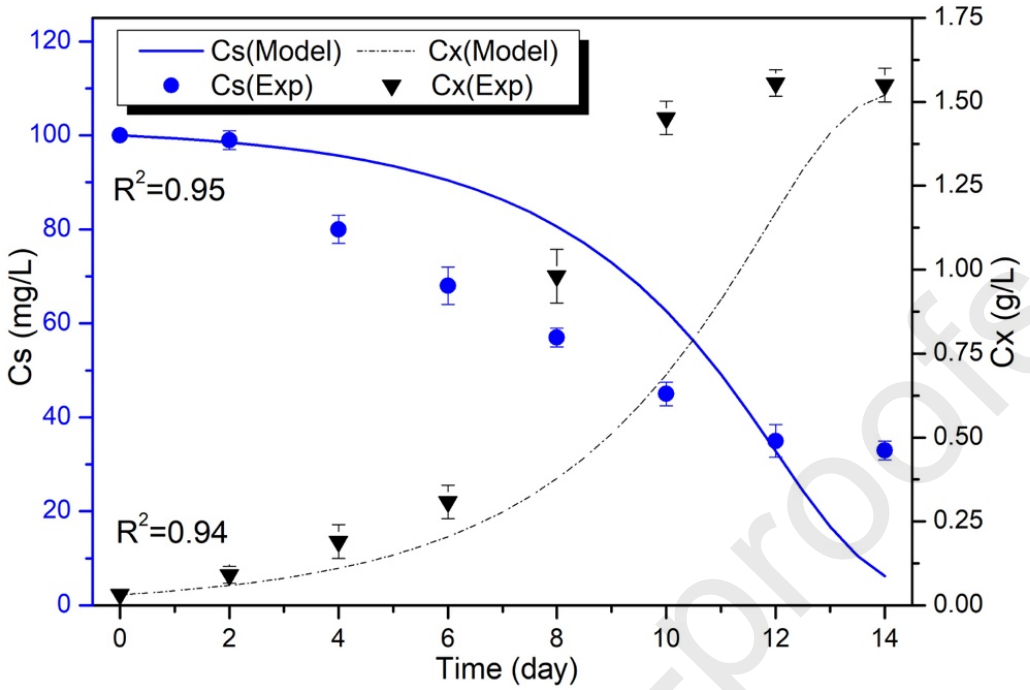

(A)

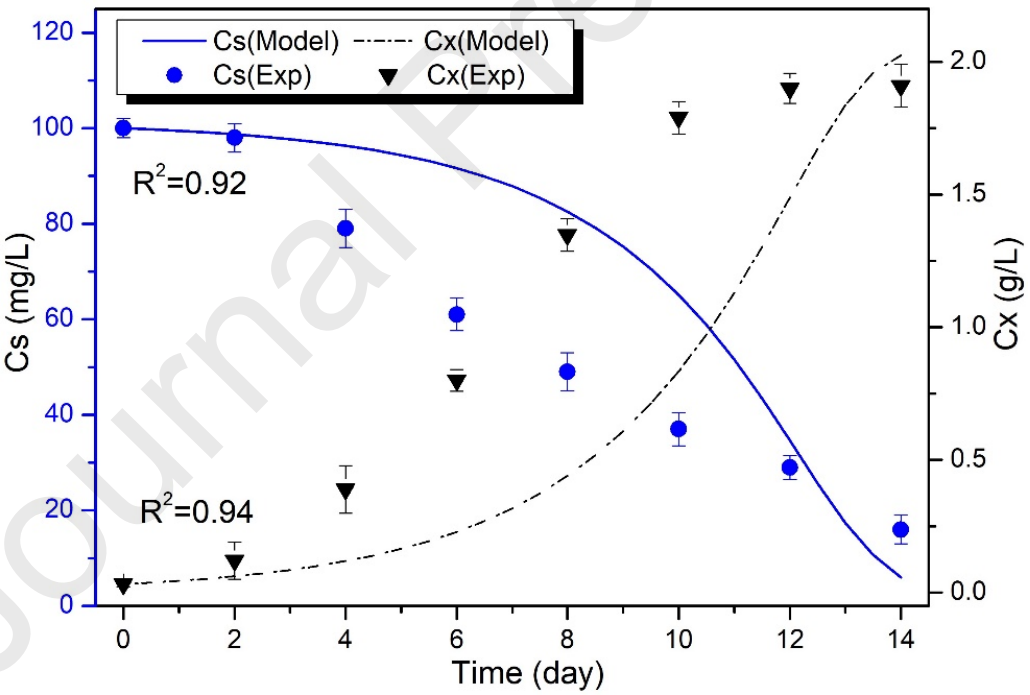

(B)

Figure 3. Experimental and stimulated time profiles of biomass concentration (C_x) and substrate concentration (C_s) in control (mechanical shaking) [A] and test (sonication at 10% duty cycle experiments [B].

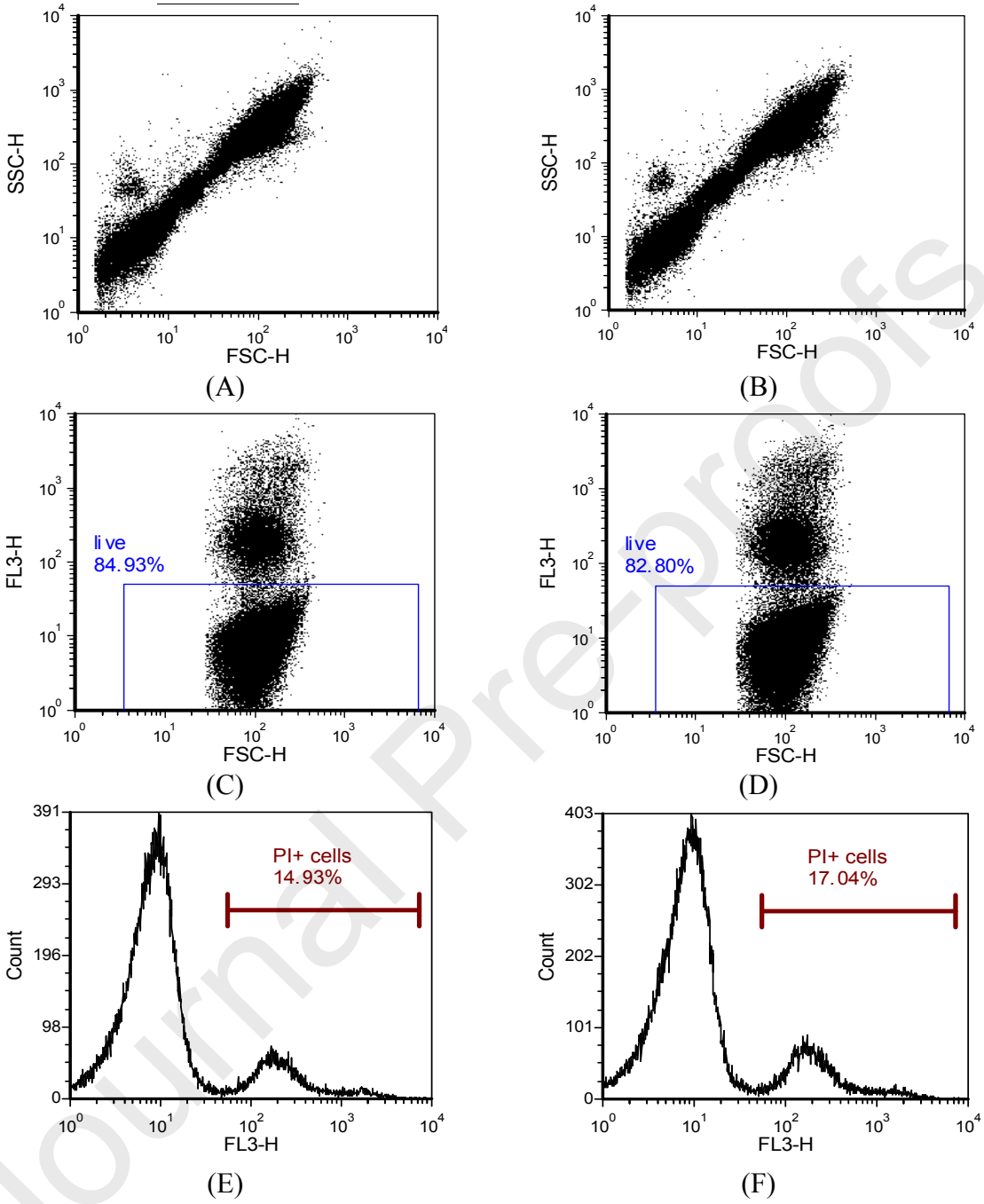

Figure 4. Flow cytometric analysis for detection of morphological changes in *C. tropicalis* cells after exposure to ultrasound. (A) and (B): Acquisition dot plots (FSC vs. SSC) of *C. tropicalis* cells for control and test experiments, respectively. (C) and (D): Acquisition dot plots (FSC vs. FL3) showing percentage of live cells present in both control and test. (E) and (F): Histogram plots (FL3 vs. count) showing dead *C. tropicalis* cells in control and test samples, respectively.

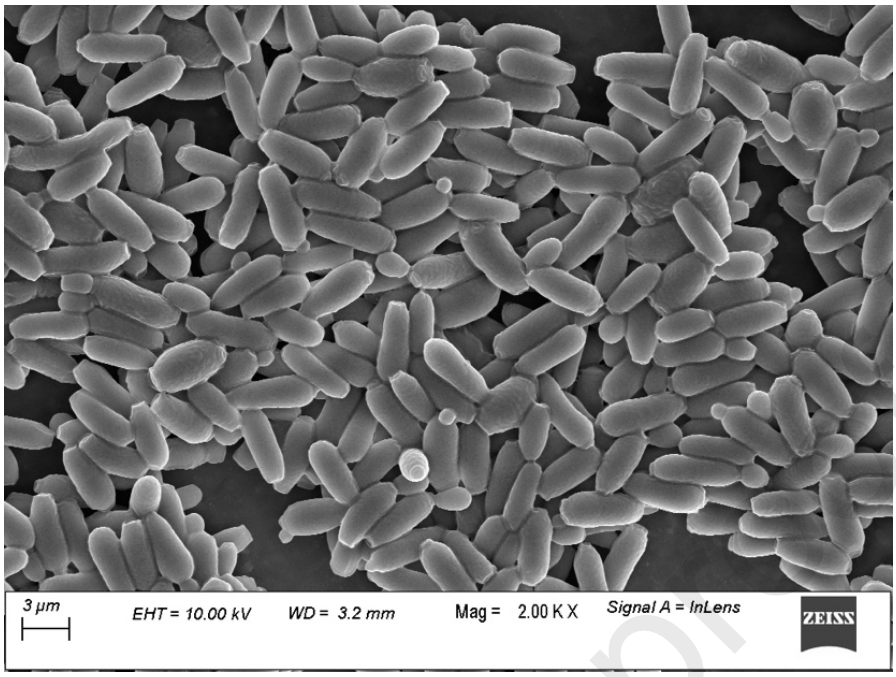

(A)

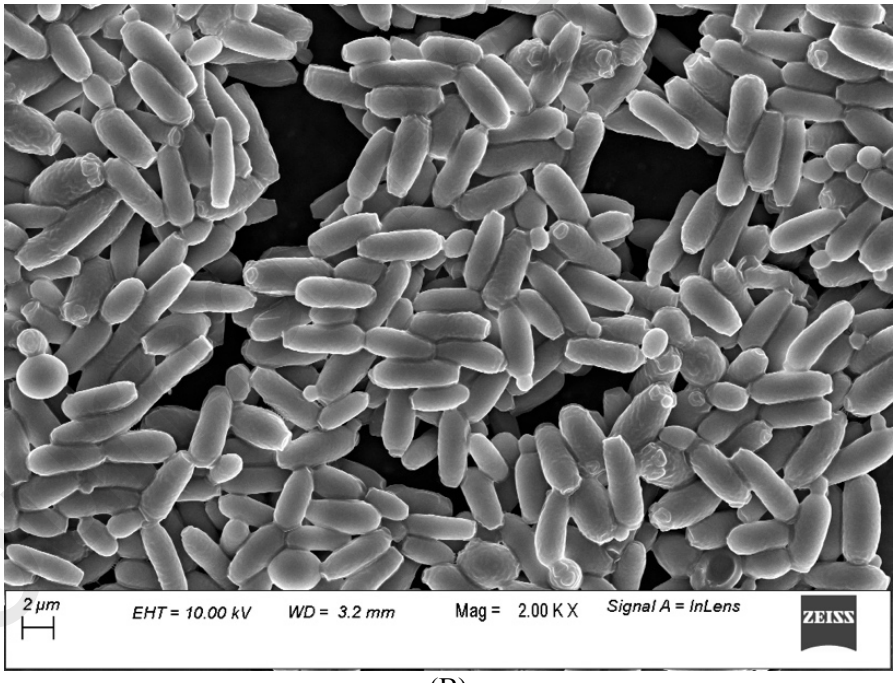

(B)

Figure 5. FE-SEM micrographs of *C. tropicalis* cells after biodegradation experiments in Control (A) and Test (B) experiments.

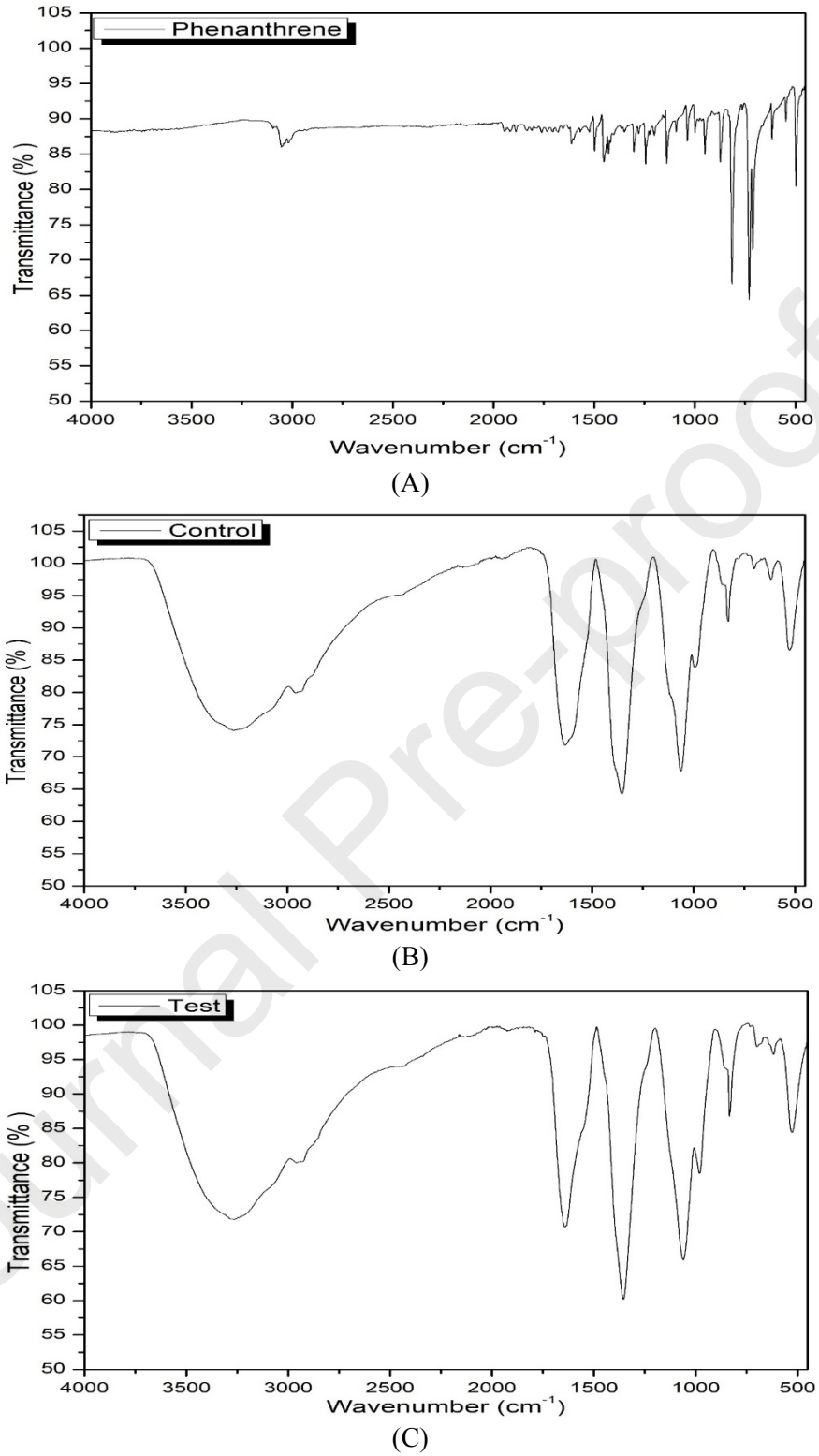

Figure 6. FTIR spectra of (A) Phenanthrene, (B) Control experiment and (C) Test experiment.

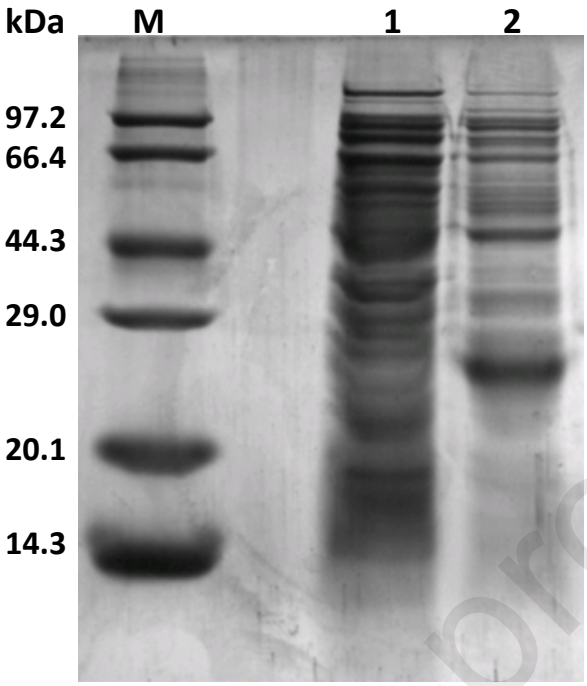

Figure 7. Lane M shows the protein molecular weight marker (Low) (97.2 kDa to 14.3 kDa), Lane 1 and Lane 2 shows the bands of test (sonicated) and control samples respectively indicating the sizes of proteins.

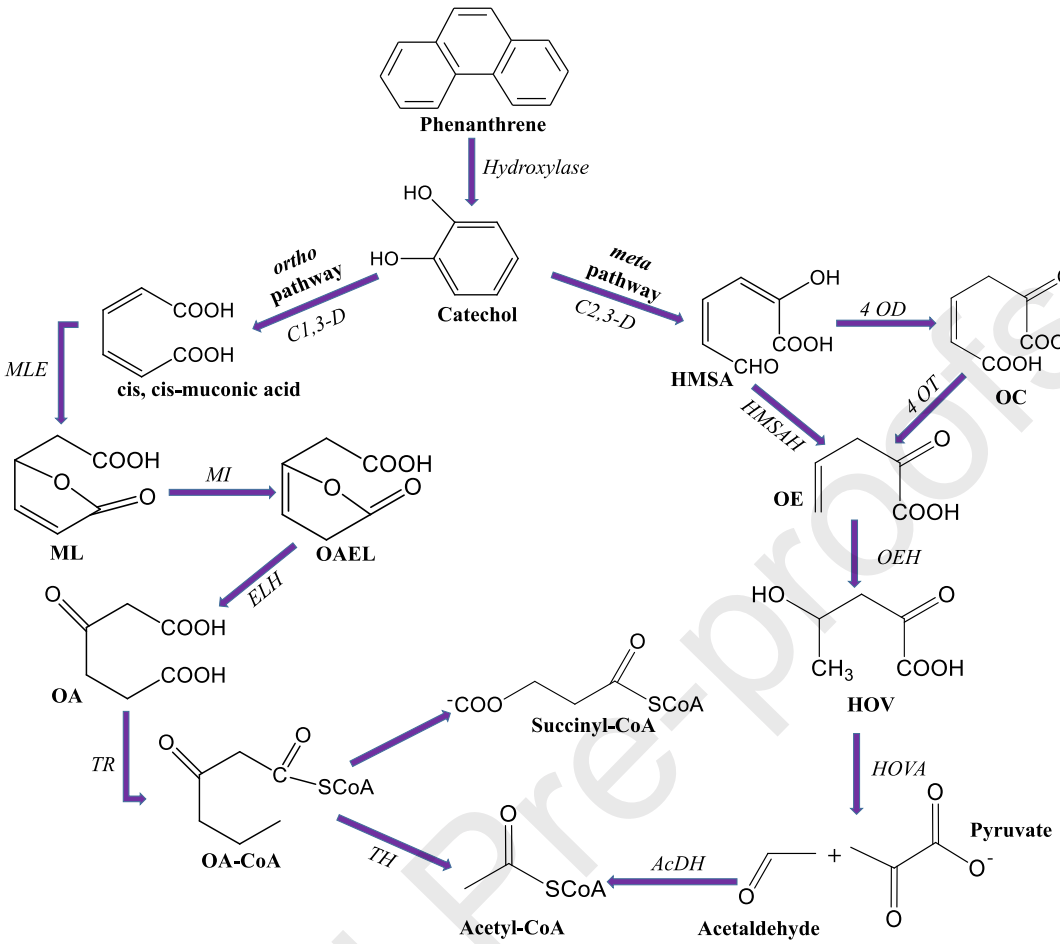

Figure 8. Aerobic degradation pathway for phenanthrene [11], [24]
Notation: C1,3–D = catechol 1,2–dioxygenase, C2,3–D = catechol 2,3–dioxygenase, HMSA = 2–hydroxymuconic semialdehyde (HMSA), ML = muconolactone, MLE = cis,cis–muconate lactonizing enzyme, OAEL = 3–oxo adipate enol–lactone, MI = mucono– lactone isomerise, OA = 3–oxo adipate, ELH = 3–oxo adipate enol–lactone hydrolase, OA–CoA = 3–oxo adipyl–CoA, TR = 3–oxo adipate succinyl–CoA transferase, TH = 3–oxo adipate CoA thiolase, HMSAH = HMSA hydrolase, 4OT = 4–oxalocrotonate tautomerase, OE = 2–oxopent–4– dienoate, 4OD = 4–oxalocrotonate decarboxylase, HOV = 4–hydroxy–2–oxovalerate, OEH = OE hydratase, HOVA = HOV aldolase, AcDH = acetaldehyde dehydrogenase.

Research Highlights

- Biodegradation of polycyclic aromatic hydrocarbon Phenanthrene using yeast, *Candida tropicalis*
- Statistical optimization of process parameters and kinetic analysis with Haldane model
- Sonication at 33 kHz and 10% duty cycle enhanced phenanthrene removal by 25%
- Overexpression of intracellular proteins during sonication analysed by SDS-PAGE
- Degradation of phenanthrene occurred via *meta* route catalysed by C2,3-D enzyme

Declaration of interests

The authors declare that they have no known competing financial interests or personal relationships that could have appeared to influence the work reported in this paper.

Niharika Kashyap
Kuldeep Roy
V.S.Moholkar

SUPPLEMENTARY MATERIAL

Mechanistic investigations in ultrasound-assisted bioremediation of phenanthrene

Niharika Kashyap,[1] Kuldeep Roy[2] and Vijayanand S. Moholkar[1,2,*]

[1] Center for the Environment, [2] Department of Chemical Engineering

Indian Institute of Technology Guwahati

Guwahati – 781 039, Assam, India

* Author for correspondence. E-mail: vmoholkar@iitg.ac.in, Fax: +91 361 258 2291

Table S1. Full factorial central composite design matrix of 4 degradation parameters in coded and actual (in parentheses) values

Run order	Medium pH (X_1)	Temperature (°C) (X_2)	Shaking speed (rpm) (X_3)	Inoculum size (%,v/v) (X_4)	Phenanthrene degraded (%)	
					Experimental	Predicted
1	0 (6)	–α (10)	0 (150)	0 (7.5)	25.50±0.07	25.64
2	0 (6)	0 (30)	0 (150)	–α (2.5)	34.00±0.16	34.39
3	–1 (4)	+1 (40)	–1 (130)	+1 (10.0)	40.50±0.09	40.85
4	0 (6)	0 (30)	0 (150)	0 (7.5)	61.00±0.30	60.85
5	+1 (8)	+1 (40)	–1 (130)	+1 (10.0)	48.50±0.19	48.66
6	–1 (4)	+1 (40)	+1 (170)	+1 (10.0)	46.00±0.09	46.16
7	–1 (4)	–1 (20)	–1 (130)	–1 (5.0)	36.00±0.28	36.02
8	+1 (8)	+1 (40)	+1 (170)	+1 (10.0)	54.00±0.03	54.10
9	+1 (8)	–1 (20)	–1 (130)	+1 (10.0)	34.50±0.06	34.93
10	–1 (4)	–1 (20)	–1 (130)	+1 (10.0)	37.00±0.16	36.75
11	0 (6)	0 (30)	0 (150)	0 (7.5)	61.00±0.28	60.85

12	–1 (4)	+1 (40)	–1 (130)	–1 (5.0)	43.00±0.17	42.75
13	–1 (4)	+1 (40)	+1 (170)	–1 (5.0)	42.00±0.10	41.68
14	0 (6)	0 (30)	+α (190)	0 (7.5)	62.00±0.09	62.06
15	–α (2)	(0 30)	0 (150)	0 (7.5)	23.00±0.07	23.31
16	+1 (8)	–1 (20)	+1 (170)	+1 (10.0)	41.00±0.14	41.25
17	+α (10)	0 (30)	0 (150)	0 (7.5)	20.50±0.19	20.06
18	–1 (4)	–1 (20)	+1 (170)	+1 (10.0)	43.00±0.23	42.93
19	+1 (8)	–1 (20)	–1 (130)	–1 (5.0)	25.00±0.38	24.83
20	0 (6)	0 (30)	0 (150)	0 (7.5)	60.50±0.21	60.85
21	0 (6)	0 (30)	0 (150)	0 (7.5)	61.00±0.13	60.85
22	0 (6)	0 (30)	0 (150)	0 (7.5)	61.00±0.09	60.85
23	+1 (8)	–1 (20)	+1 (170)	–1(5.0)	25.00±0.06	24.77
24	0 (6)	0 (30)	0 (150)	+α (12.5)	49.50±0.09	48.97
25	0 (6)	+α (50)	0 (150)	0 (7.5)	45.50±0.08	45.22
26	+1 (8)	+1 (40)	+1 (170)	–1 (5.0)	40.00±0.12	40.25
27	0 (6)	0 (30)	–α (110)	0 (7.5)	57.00±0.17	56.81
28	0 (6)	0 (30)	0 (150)	0 (7.5)	60.50±0.15	60.85
29	0 (6)	0 (30)	0 (150)	0 (7.5)	61.00±0.26	60.85
30	+1 (8)	+1 (40)	– 1 (130)	–1 (5.0)	41.00±0.36	41.18
31	–1 (4)	–1 (20)	+1 (170)	–1 (5.0)	36.00±0.09	35.83

Table S2. Statistical analysis of central composite experimental design for process parameter optimization of phenanthrene degradation

(A) Model Coefficients, *t*− and *p*−values for each variable

Model term	Coefficient	*t*-value	*p*-value
Intercept (β_0)	60.857	445.894	0.000*
Linear coefficients			
Medium pH (X_1)	-0.812	-11.023	0.000*
Temperature (X_2)	4.895	66.421	0.000*
Roto speed (X_3)	1.312	17.806	0.000*
% Inoculum (X_4)	3.645	49.462	0.000*
Square coefficients			
Medium pH (X_1) × Medium pH (X_1)	-9.792	-145.014	0.000*
Temperature (X_2) × Temperature (X_2)	-6.354	-94.109	0.000*
Rotor speed (X_3) × Rotor speed (X_3)	-0.354	-5.256	0.000*
% Inoculum (X_4) × % Inoculum (X_4)	-4.792	-70.970	0.000*
Interaction coefficients			
Medium pH (X_1) × Temperature (X_2)	2.343	25.962	0.000*
Medium pH (X_1) × Rotor speed (X_3)	0.031	0.346	0.734
Medium pH (X_1) × % Inoculum (X_4)	2.343	25.962	0.000*
Temperature (X_2) × Rotor speed (X_3)	-0.218	-2.423	0.028*
Temperature (X_2) × % Inoculum (X_4)	-0.656	-7.269	0.000*
Rotor speed (X_3) × % Inoculum (X_4)	1.593	17.654	0.000*

* Significant *p* values, $p \leq 0.05$; R^2= 0.999; Predicted R^2 = 0.998; Adjusted R^2 = 0.999.

(B) ANOVA for quadratic model

Source	DF	SS	MS	*F*-value	*p*-value
Regression	14	5109.90	364.99	2799.15	0.000
Linear	4	951.46	237.86	1824.19	0.000
Square	4	3929.60	982.40	7534.06	0.000
Interaction	6	228.84	38.14	292.50	0.000
Residual (error)	16	2.09	0.13		
Lack of fit	10	1.73	0.17	2.91	0.102
Pure Error	6	0.36	0.06		
Total	30	5111.98			

DF – Degree of freedom; SS – Sum of squares; MS – Mean square

(C) Analysis of contour plots: Parameter space for maximum phenanthrene degradation

Contour plot	Range of parameter				
	Medium pH (X_1)	Temperature (X_2)	Rotor speed (X_3)	Inoculum size (X_4)	Phenanthrene degraded (%)
a. (X_2) vs (X_1)	5.10-6.90	28.00-38.00	150#	7.50#	60.00
b. (X_3) vs (X_1)	4.90-6.80	30#	138.00-190.00	7.50#	60.00
c. (X_4) vs (X_1)	5.20-6.80	30#	150#	6.80-9.70	60.00
d. (X_3) vs (X_2)	6#	20.70-40.00	127.00-190.00	7.50#	60.00
e. (X_4) vs (X_2)	6#	20.75-38.30	150#	6.80-10.20	60.00
f. (X_3) vs (X_4)	6#	30#	130.50-190.00	6.50-11.50	60.00

Centre point values of process parameters

Global optimum values of variables: medium pH = 6.20, temperature = 33.43°C, agitation speed = 190 rpm, % inoculum = 9.26 vol%, % phenanthrene degraded = 65.19%.

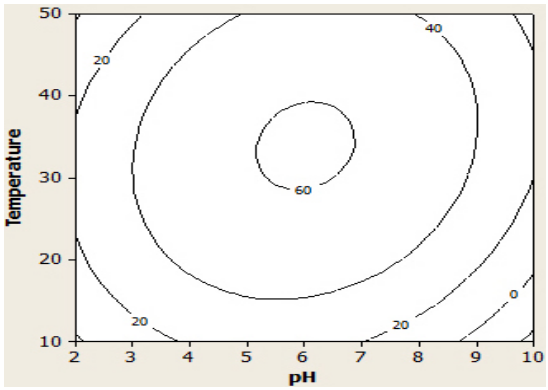

(A)

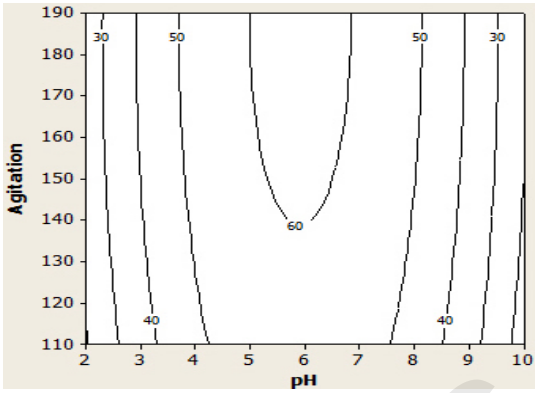

(B)

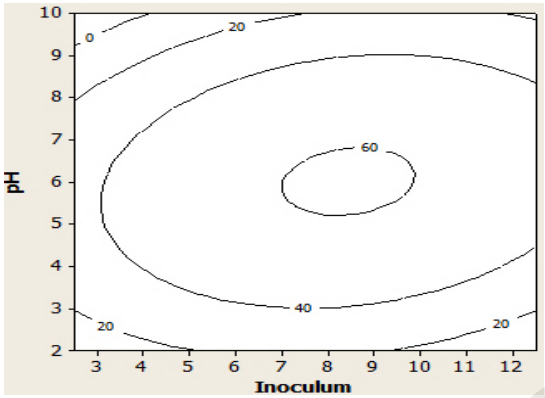

(C)

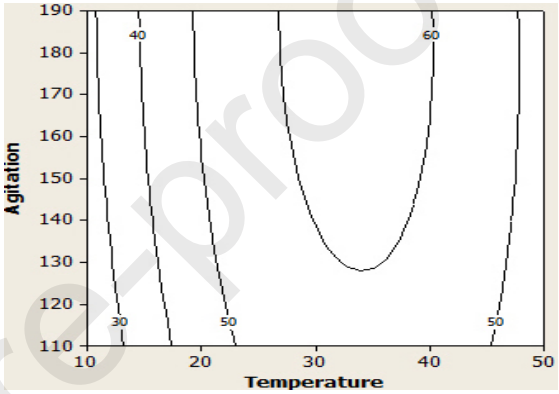

(D)

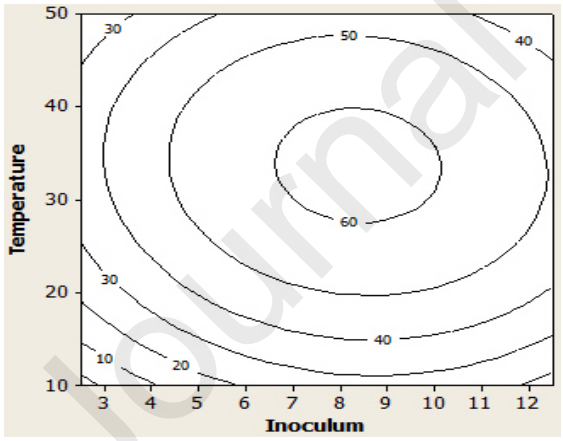

(E)

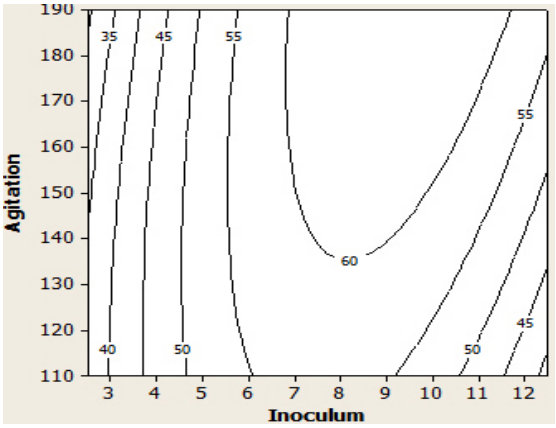

(F)

Figure S1. Contour plots depicting interactions among different process parameters for phenanthrene degradation. (A) Temperature and medium pH, (B) Agitation and medium pH, (C) Inoculum size and medium pH, (D) Agitation and temperature, (E) Inoculum size and temperature, (F) Inoculum size and agitation.

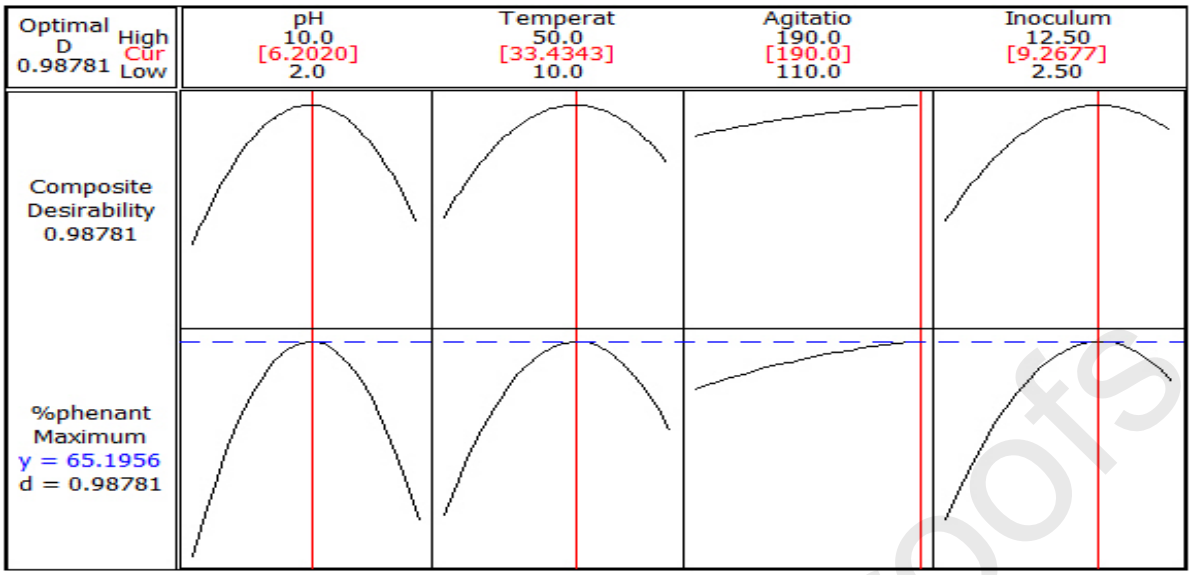

Figure S2. Optimization plots depicting the global optimum parameters for phenanthrene biodegradation. Global optimum values of variables: medium pH = 6.2, temperature = 33.4°C, agitation speed = 190 rpm, % inoculum = 9.26 vol%, % phenanthrene degraded = 65.19%.

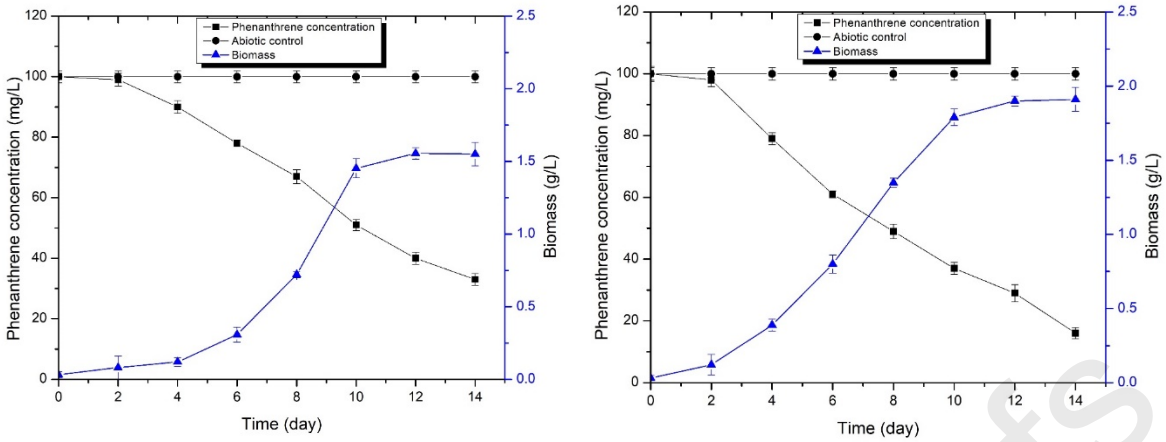

Figure S3. (A) Profiles of validation experiments for results of optimization by central composite design. (B) Profiles of validation experiments with mechanical agitation replaced with sonication at 10% duty cycle. Abiotic control (●) profiles are also shown.

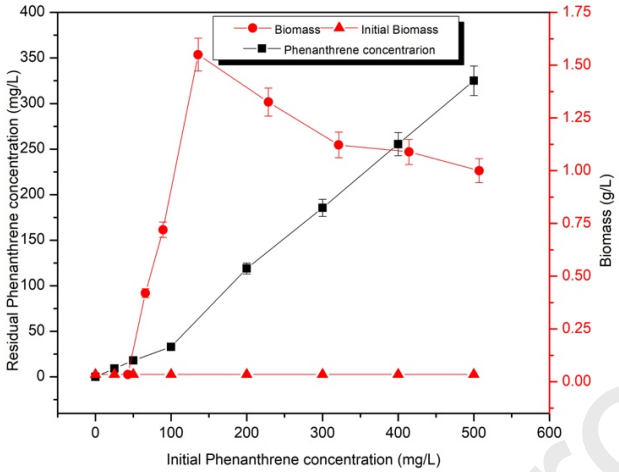

Figure S4. Biomass growth and phenanthrene degradation after 14 days of batch biodegradation under different initial concentration of phenanthrene (0 – 500 mg L^{-1})

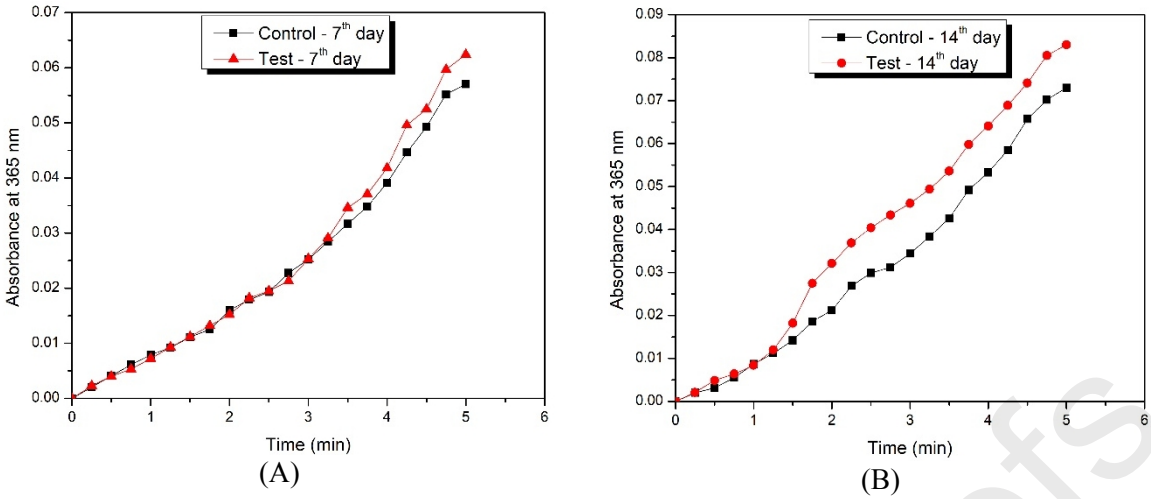

Figure S5**.** Change of absorbance with respect to time during catechol 2,3-dioxygenase assay. Fig:(A) indicates increase in absorbance on 7th day of control and test experiments and Fig: (B) indicates increase in absorbance 14th day of control and test experiments.

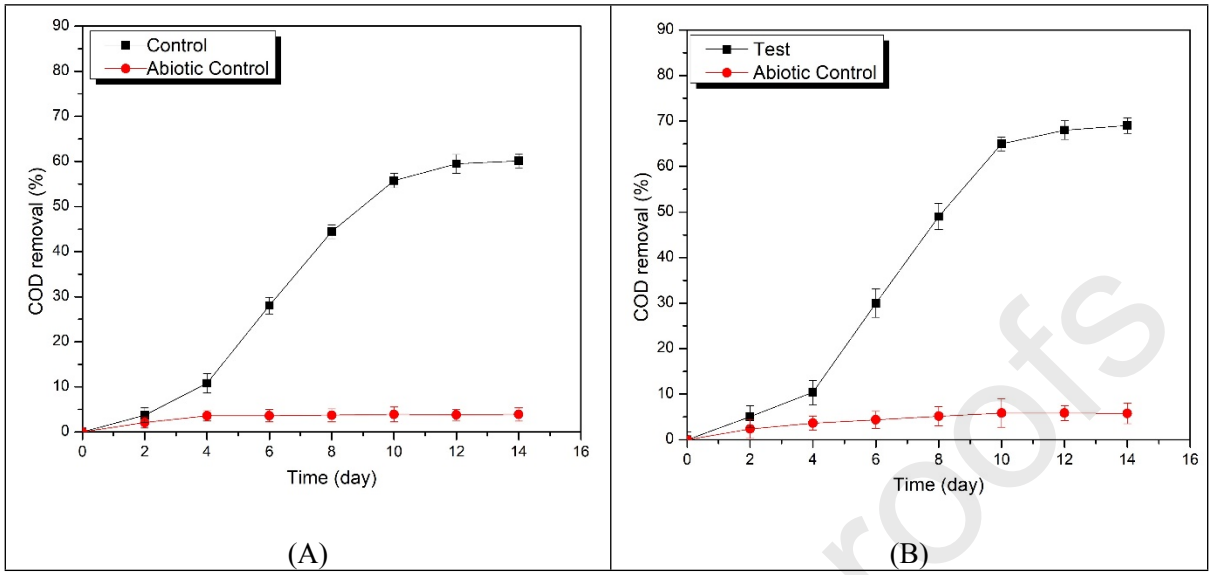

Figure S6. Percentage removal of COD after biodegradation experiment. (A) Control and (B) Test.